



Citation for published version:

Gursul, I & Wang, Z 2018, 'Flow control of tip/edge vortices', *AIAA Journal*, vol. 56, no. 5, pp. 1731-1749.
<https://doi.org/10.2514/1.J056586>

DOI:

[10.2514/1.J056586](https://doi.org/10.2514/1.J056586)

Publication date:

2018

Document Version

Peer reviewed version

[Link to publication](#)

University of Bath

Alternative formats

If you require this document in an alternative format, please contact:
openaccess@bath.ac.uk

General rights

Copyright and moral rights for the publications made accessible in the public portal are retained by the authors and/or other copyright owners and it is a condition of accessing publications that users recognise and abide by the legal requirements associated with these rights.

Take down policy

If you believe that this document breaches copyright please contact us providing details, and we will remove access to the work immediately and investigate your claim.

Flow Control of Tip/Edge Vortices

Ismet Gursul & Zhijin Wang

University of Bath, UK

Abstract

Location, strength and structure of tip and edge vortices shed from wings and bodies can be manipulated by using flow control techniques. Flow physics of these approaches involve flow separation from the edge, roll-up into the vortex, wing flow regime, vortex instabilities, vortex-vortex interactions, and vortex-turbulence interactions. Actuators include continuous and unsteady blowing and suction, bleed, and control surfaces, which add momentum, vorticity and turbulence into the vortices. It is noted that actuation may have effects on more than one aspect of the flow phenomena. A comparative review of the control of delta wing vortices, tip vortices, and afterbody vortices is presented. The delay of vortex breakdown and the promotion of flow reattachment require different considerations for slender and nonslender delta wings, and may not be possible at all. Tip vortices can be controlled to increase the effective span, to generate rolling moment, to attenuate wing-rock, and to attenuate vortex-wing interactions. While there are different approaches for each application, opportunities for future research on turbulence ingestion, bleed, and excitation of vortex instabilities exist. Recent research also indicates that active and passive flow control can be used to manipulate the afterbody vortices in order to reduce the drag.

I. Introduction

It is desirable to modify the location, trajectory, and structure of the tip or edge vortices shed from wings and bodies in various aerospace applications. Three examples of the tip or edge vortices are shown in Figure 1. They are a tip vortex over a large aspect ratio wing [1], a pair of leading-edge vortices over a slender delta wing [2], and afterbody vortices of an axisymmetric cylinder with a slanted base [3]. Depending on the objectives, the approach to flow control may be different. The objectives may vary from lift enhancement, drag reduction, flight control, attenuation of limit-cycle wing motion, to the prevention of the interaction of vortices with downstream surfaces that may otherwise cause buffeting, noise, and undesired forces or moments. Consequently, the strategies for vortex control widely vary, and may even become opposite in different applications. For example, while it is desirable to strengthen the vortex and move it closer to the surface in some applications, such as in lift enhancement and flight control of delta wings, the opposite objective is pursued in some other cases such as in the control of afterbody vortices to reduce the drag. One can also have different strategies for the desired structure of the vortex core. While a compact and coherent vortex is desirable in many cases, a diffused and incoherent vortex may be a more favourable option for certain applications such as wake hazard and vortex-blade interaction.

This review article starts with a discussion of the flow physics of vortex control techniques. We discuss the following parameters and flow phenomena relevant to the flow control philosophy: the leading-edge separation and vortex formation, vortex strength (circulation) and swirl ratio, external pressure gradient, wing flow, vortex breakdown, vortex instabilities, interaction of multiple vortices, and turbulence ingestion into the vortex core. The discussion of these aspects also includes the coupling between them, which may or may not be favourable for the objectives of vortex control. The simplest example is that stronger vortex is needed for lift enhancement on a delta wing, but this may trigger vortex breakdown, which in turn may cause a decrease in the lift force.

Subsequently, we continue with a discussion of the flow control methods that modify the main parameters or exploit the vortex phenomena in order to achieve the desired objectives. These are continuous blowing and suction, unsteady blowing (pulsed jets and synthetic jets), small aspect ratio jets, bleed, plasma actuators, control surfaces, and controlled roughness. Finally, a critical review of the following categories of vortex control is presented, comparing

the effects of various flow mechanisms and actuation methods: control of delta wing vortices, control of tip vortices of high aspect ratio wings, attenuation of wing-rock, attenuation of wake hazard of large aircraft, vortex-rotorcraft blade interaction, fin buffeting, and drag reduction of afterbody vortices.

II. Flow Phenomena and Parameters

A. Separation and vortex formation

This stage is undeniably the most important aspect of vortex control strategies. Three-dimensional shear layers separate at the leading-edge and roll up into concentrated vortices as schematically shown in Figure 2(a). The geometry of the edge, hence the separation line, may significantly affect the development of the vortical flow. The angle of attack α and the sweep angle Λ are the most important parameters for fixed separation lines (sharp leading-edges). For rounded leading-edges, the leading-edge shape offers some potential in flow control applications. For example, the Coanda effect can be exploited to direct the shear layer inboard of the wing.

While the separated shear layer can be oriented in various directions at the leading-edge by flow control, it is more difficult to predict and control the roll-up process into the concentrated vortex. Figure 2(b) schematically shows the roll-up process, which is dominated by the Kelvin-Helmholtz instability [4-6]. This instability is observed when the Reynolds number based on the chord length is on the order of $Re \approx 10^4$. The instantaneous shear layer sketched in Figure 2(b) leads to a well-defined concentrated vortex in the time-averaged sense. The excitation of the shear layer instability is likely to affect the roll-up process and the properties of the time-averaged vortex. This will be further discussed later on.

Strong swirl (tangential) velocity and jet-like axial velocity are typical in tip/edge vortices. The influence of the swirl velocity on the axial velocity can be seen by the simple model of Batchelor [7]. Neglecting the growth of the vortex in the axial direction and assuming steady axisymmetric vortex, the quasi-cylindrical equation of motion in the radial direction reduces to [7,8]:

$$\frac{V_{\theta}^2}{r} = \frac{1}{\rho} \frac{\partial p}{\partial r} \quad (1)$$

When integrated between the edge of the vortex core and the axis ($r = 0$), this equation predicts a pressure decrease at the vortex axis as the integral is positive:

$$\frac{p_{\infty} - p_{r=0}}{\rho} = \int_0^{\infty} \frac{V_{\theta}^2}{r} dr \quad (2)$$

Batchelor [7] used the Bernoulli equation to predict the axial velocity U at $r = 0$:

$$U_{r=0}^2 = U_{\infty}^2 + 2 \int_0^{\infty} \frac{V_{\theta}^2}{r} dr \quad (3)$$

As the integral is positive, one expects a faster axial flow at the vortex axis. The maximum axial velocity can be as large as four or five times the freestream velocity for slender delta wing vortices. When the viscous flow is considered, the axial velocity decreases due to the losses. It is clear that both the swirl velocity profile and the viscous losses can be effective for manipulating the streamwise variation of the axial velocity.

B. Vortex circulation and swirl ratio

The circulation of the time-averaged vortex grows in the chordwise direction as a result of continuous feeding of the vorticity from the separated shear layer. The simplest case is the axisymmetric conical vortex proposed by Hall [9] and experimentally confirmed over slender delta wings. In this model, the circulation increases linearly in the streamwise direction for the conical vortex. In other cases, such as for the afterbody vortices [3], the variation of the circulation is strongly nonlinear and increases much faster initially. From the point of view of

flow control, increased circulation (or swirl velocity) is desired if one wishes to achieve increased lift on the wing.

An important parameter is the swirl ratio (or swirl angle, $\phi = \tan^{-1}(V_\theta/U)$), which can be defined as the ratio of the swirl velocity to the axial velocity. This parameter is believed to play an important role for the onset of vortex breakdown. Hall [8] suggests that, when the maximum swirl angle reaches about 50 degrees, vortex breakdown occurs. Another important parameter, q is used in the definition of the Q-vortex, which is the ratio of the maximum swirl velocity to the axial velocity defect at the axis:

$$q = \frac{\Gamma}{2\pi r \Delta u} \approx 1.57 \frac{V_{\theta max}}{\Delta u} \quad (4)$$

The parameter q is always larger upstream of breakdown (jet-like axial velocity) than that downstream (wake-like axial flow).

C. External pressure gradient

The tip/edge vortices are subject to highly non-axisymmetric external pressure gradient. Small or negligible streamwise pressure gradient exists above and outboard of the wing, while there are significant pressure gradients inboard and below due to the wing. Hall [8] showed that any external pressure gradient outside of the vortex core can be amplified at the vortex axis. From Equation (1), the difference between the axial pressure gradient at the axis and any arbitrary radial point can be expressed as:

$$\left(\frac{\partial p}{\partial z}\right)_{r=0} - \left(\frac{\partial p}{\partial z}\right) = - \int_0^r \frac{\partial}{\partial z} \left(\frac{\rho V_\theta^2}{r}\right) dr \quad (5)$$

This shows that the pressure gradient along the axis will be different than the pressure gradient outside of the vortex core. The difference depends on the square of the swirl velocity, hence the square of the circulation. Hall suggested that the pressure gradient along

the vortex axis becomes more adverse. Thus, if the circulation is increased by flow control, this may cause an earlier vortex breakdown as discussed later on.

D. Wing flow

The flow regime over the wing (attached or stalled) has a significant effect on tip vortices. This is schematically shown for tip vortices over a large aspect ratio wing in Figure 3(a). While there is flow reattachment on the wing at small angles of attack, this is not possible for a stalled wing flow at high angle of attack. However, one has the advantage that the location and structure of the tip vortex can be manipulated by separation control of the wing flow, which is separated at the leading-edge in this example. Delay of flow separation on the wing offers greater potential for the control of the tip vortex than the case of attached wing flow.

There is a similar case over delta wings as shown in Figure 3(b). For small angles of attack or low sweep angles (nonslender delta wings), the flow reattaches on the wing. On the contrary, for larger angles of attack or high sweep angles (slender delta wings), there is no flow reattachment on the wing surface. Consequently, separation control is unlikely to be effective for slender delta wings.

E. Vortex breakdown

With increasing angle of attack of a delta wing, the vortices undergo a sudden expansion, accompanied by the deceleration of the axial velocity, known as vortex breakdown as sketched in Figure 4. Vortex breakdown has adverse effects on the time-averaged lift and pitching moment. In addition, force/moment fluctuations caused by the unsteady nature of vortex breakdown may have an impact on aircraft stability and control. Vortex breakdown may also cause wing and fin buffeting.

Both experiments and theoretical models [8,10-12] confirm that there are essentially two main parameters that determine whether the vortex breakdown will occur or not, as discussed in [13]. These are swirl level and external pressure gradient. In fact, the effect of these parameters can be already seen from the simple model discussed by Equation (5). Sufficiently large adverse pressure gradient can develop on the axis if the external pressure gradient is made slightly more adverse or the swirl velocity is increased. An increase of the swirl level or the pressure gradient promote an earlier breakdown, moving it to a more upstream location. If it is desired to delay vortex breakdown or eliminate it completely, one needs to decrease the

swirl level of the vortex or make the pressure gradient less adverse. The latter can be achieved by adding momentum in the axial direction. Likewise, this can be achieved by applying suction along the vortex axis at a location downstream of the onset of vortex breakdown [14]. In the case of blowing from the leading-edge of the wing, depending on the direction and introduction of blowing, there might be an effect on the swirl velocity as well. If blowing causes an increase in the swirl velocity, the desired outcome of delayed breakdown may not occur, even if the pressure gradient alone is made less adverse.

F. Vortex instabilities

As discussed earlier, the Kelvin-Helmholtz instability is the essential part of the vortex roll up and the excitation of this instability may be effective for controlling the formation process and also for promoting the reattachment of the flow on the wing surface. Other vortex instabilities may also be important for flow control purposes. For example, the helical mode instability downstream of the vortex breakdown [15], which also manifests itself as the spiral type of breakdown (see Figure 4), is a well-known vortex instability. Normally, one wishes to eliminate the quasi-periodicity of the flow due to this instability as it provides the excitation for wing and fin buffeting. The promotion or excitation of this instability has not been tried in wing flows, however it may have the potential to achieve diffused trailing vortices in the wake. The excitation of the helical mode instability has increased the spreading of a swirling jet [16], suggesting potential for its use in other vortex flows.

Even in the absence of breakdown, vortex flows can be highly unsteady. Although the source of meandering of trailing vortices in the far wake has been much debated, the vortex roll-up process is clearly behind similar observations of meandering of tip/edge vortices over wings. In fact, the similarity of meandering behavior is illustrated in the three different types of vortex flows in Figure 5. These are trailing tip vortices in the wake [17], delta wing vortices [2] and afterbody vortices [3]. The meandering mode has been captured by means of the Proper Orthogonal Decomposition analysis as shown in Figure 5. The most energetic mode exhibits a vortex dipole centered on the time-averaged vortex. The second most energetic modes (not shown here) are also vortex dipoles that are orthogonal to those in the first modes. A linear combination of these eigenmodes represents displacements of the vortex core in the azimuthal wavenumber $m = 1$. This mode has a very large wavelength, corresponding to very low Strouhal numbers (on the order of 10^{-2} to 10^{-1}) based on the wing chord length. This

range is typical for unsteady aerodynamics of maneuvering wings and deformation of aeroelastic flexible wings. Hence potential applications of vortex control exist.

G. Interaction of multiple vortices

Tip/edge vortices form as counter-rotating pairs in flight and the separation distance between them is directly related to the wing span. The vortex pair travels downstream and downwards due to the induced velocity of the pair. The ratio of the vortex radius a to the vortex separation distance b is an important parameter with regard to the instabilities of vortex pairs [18]. According to the studies of parallel vortex pairs, both long wavelength and short wavelength instabilities can be amplified. For the long wavelength (Crow) instability, the most unstable wavelengths are between $\lambda/b \approx 6$ and 8 for $0.1 \leq a/b \leq 0.3$. On the other hand, it is expected that the short wavelength (elliptic) instability scales on the core radius. For parallel vortex pairs in the range of $0.1 \leq a/b \leq 0.3$, the counter-rotating vortex pair becomes unstable above a critical Reynolds number Γ/v , which is on the order of 10^2 to 10^3 .

The stability of developing non-parallel vortex pairs on the wings and bodies is less understood. For example, for the conical pairs over slender delta wings, both the vortex radius a and vortex separation distance b increase linearly in the streamwise direction. The symmetry breaking on delta wings has some similarity to the well-known vortex asymmetry on bodies of revolution [19]. Keener and Chapman [20] suggested that the vortex pair asymmetry on slender bodies of revolution and slender delta wings is created by the same “hydrodynamic instability” resulting from the “crowding” together of the vortices. In the case of bodies of revolution, it was suggested that a convective instability of the originally symmetric flow causes the vortex asymmetry [21,22].

Co-rotating vortices are common on wings, such as on double-delta wings, as well as in the wakes of aircraft. Hence vortex merging and its control (promotion or delay) can be an effective method for controlling vortex flows. For equal strength co-rotating vortices, experiments and simulations confirm that vortex merging takes place when a/b is less than a critical value (0.24 to 0.29) [23], depending on the Reynolds number. Decrease in separation distance b and increase in vortex core radius a accelerate the vortex merging process. Although it is more difficult to predict the critical value of a/b for merging of the unequal strength co-rotating vortices, the effect of decreasing separation distance and increasing

vortex core radius is expected to be similar, i.e. promotion of merging.

H. Turbulence ingestion

Most of the studies related to the effect of turbulence ingestion into the vortex cores are on the jet-vortex interaction, although the turbulence can also be generated by some other means, for example by producing flow separation with mini-spoilers near the vortices. With regard to the jet-vortex interaction, which is of interest for flow control by blowing, the effect mainly depends on the jet momentum coefficient, the distance between the jet and the vortex core, and the orientation of the jet. Even for the large distances between co-flowing jets and vortices, jet and turbulence ingestion into the vortex core has been observed in experiments [24] as shown in Figure 6(a). As the jet turbulence (red) travels downstream, it is also stretched and rotated around the vortex (yellow), wrapping around and penetrating into the core. When the jet is initially closer to the vortex, the interaction and turbulence ingestion are faster. Figure 6(b) shows that the effect of blowing on the time-averaged crossflow velocity can be significant. It is noted that this effect is not an artefact of the meandering, since the instantaneous velocity magnitude is also decreased significantly. Experiments [25] and simulations [26] show that, when the jet is blowing very near the core, the tip vortex diffuses rapidly (but maintains its circulation). There is significant effect on the turbulence ingestion even for small incidences between the jet and the vortex [24]. When the jet is not parallel to the vortex axis, and is introduced tangentially near the wing tip, jet turbulence can be rapidly ingested into the vortex core [1]. This is illustrated in Figure 7 for spanwise blowing from a slot in the wing tip (Slot 3, see the inset in the figure).

Turbulence ingestion and the resulting diffused vortices can promote earlier merging of co-rotating vortices. In Figure 8, the inset shows the locations of the simulated tip and flap vortices as well as the jet nozzle [23]. Further downstream the tip and flap vortices have rotated around each other as seen in the baseline case (no jet blowing) as shown in Figure 8(a). With the jet activated ($C_{\mu}=0.05$), one observes the vortex merging process starting in the same streamwise plane (Figure 8(b)). Although the momentum coefficient in this example is rather large for flow control applications, smaller momentum coefficients are likely to be as effective when the jet is introduced closer to the vortices.

III. Flow Control Methods and Actuators

In this section we continue with a discussion of the flow control methods and actuators that modify the main parameters or exploit the vortex phenomena in order to achieve the desired objectives.

A. Continuous blowing and suction

Blowing and suction near the leading-edge offer the most effective methods if the separation of the shear layer is to be manipulated. Figure 9(a) shows examples of blowing slots near the wing tip [1]. In this case, the combination of the rounded wing tip and Slot 3 produces the Coanda effect. Each slot generates substantially different angles of separated shear layer and vortex topologies, including multiple vortices. Also, generally, blowing gives rise to additional vorticity shed, resulting in stronger vortices.

Suction near the leading-edge has also been tried to manipulate the shear layer separated at the leading-edge of a delta wing [27] [and also to delay the vortex breakdown \[28\]](#). Not only was the shear layer oriented inboard, resulting in the time-averaged vortex forming more inboard, but also the circulation of the vortex was found to decrease with suction [27]. This is due to the removal of some of the vorticity shed from the leading-edge by means of suction.

B. Unsteady blowing

Unlike continuous blowing and suction, unsteady blowing (pulsed jet or synthetic jet) aims at the excitation of the shear layer instability. Typically, the momentum coefficient is much smaller (on the order of 10^{-4} to 10^{-3}) compared to the case of continuous blowing. Figure 9(b) shows two different examples of the leading-edge slot geometry [29,30]. In spite of the major difference in the direction of unsteady blowing, both cases demonstrated substantial lift enhancement. This suggests that, for small amplitude unsteady blowing, the direction of blowing is not as critical, since the flow control relies on the excitation of the shear layer instability.

C. Small aspect ratio jets

In general, small aspect ratio jets are used to add momentum in order to delay vortex breakdown by overcoming the adverse pressure gradient. They have been located in various positions on the wing surface beneath the vortex or near the leading-edge. However, unlike

quasi-two-dimensional or large aspect ratio jets that add momentum while generating vortex sheets, small aspect ratio jets from nozzles or slots add momentum while producing significant streamwise vortices of the same sign as the primary vortex. This is similar to vortex generation by pitched and yawed jets in uniform freestream [31]. In the case of jets near the wing tip, even blowing with zero yaw angle can produce vortices due to the induced velocity field of the primary vortex. Therefore, the interaction of multiple vortices may be unavoidable. In fact, in some cases, additional vortex and its interaction with the primary vortex may be beneficial.

D. Bleed

Passive bleed exploiting the natural pressure difference between the upper and lower surfaces can be an effective method to manipulate the tip/edge vortices. Bleed slots were placed near the wing tip/edge for rectangular wings [32], delta wings [33], and double-delta wings [34]. Figure 10 shows the baseline case and three slots with different widths and distances from the wing tip for a rectangular wing [32]. (Only a spanwise distance of one-eighth of the wing span is shown in the figure). A jet-like flow from the bleed slot and a more diffused structure of the time-averaged vortex are apparent. The corresponding instantaneous vorticity fields are shown below the time-averaged vorticity fields. Small-scale vortices in the shear layer from the wing tip interact with the small-scale vortices of opposite sign from the bleed slots. For tip slot E, merging of vorticity of the same sign appears to lead to the diffused time-averaged vortex. Note that the vorticity away from the tip in the instantaneous fields is due to the wing flow separated at the leading-edge and disappears when time-averaging is performed. Incoherent and diffused tip vortices are considered to be due to the vortex interactions as well as the turbulence ingestion originating from the bleed slot.

E. Plasma actuators

As the plasma actuators produce a wall-jet, they can be used to add momentum into the vortical flows. It was found that, with the actuator placed near the apex, streamwise-oriented plasma actuators can delay vortex breakdown on a slender delta wing [35]. When the actuators were located near the leading-edge, sufficient rolling moments could be produced for a non-slender delta wing [36].

F. Control surfaces

Winglets are the most well-known stationary surfaces to passively control the tip vortices in order to reduce the induced drag [37]. Other passive surfaces include mini airfoils to produce additional vortices and mini-spoilers near the leading-edge or trailing-edge to produce turbulence and promote ingestion of turbulence into the tip vortices [38,39]. These are sketched in Figure 11(a).

Oscillating control surfaces, for example oscillating flaps, have been proposed to excite the vortex pair instabilities in order to accelerate vortex decay in aircraft wakes [40]. Oscillating leading-edge flaps on a delta wing can control the location of vortex breakdown [41] (see Figure 11(b)). Mini- and micro-flaps have been used to manipulate the flow separation from a rounded leading-edge [42]. It was shown that a small disturbance from a controlled roughness near the nose of bodies of revolution can be used to trigger or reverse the vortex asymmetry, hence providing a means to control the magnitude of the side-force [22]. The typical size of the roughness was around 1.5% of the body diameter. It was suggested that the small disturbances caused by the controlled roughness propagate due to a convective instability.

IV. Vortex Control Approaches

In this section, a critical review of various vortex control approaches for different applications is presented, comparing the effects of various flow mechanisms and actuation methods.

A. Control of delta wing vortices

Historically, much of the work was on the delay or elimination of vortex breakdown, as reviewed in [43,44]. This is more relevant to the slender delta wings ($\Lambda \geq 65^\circ$) for which the contribution of the leading-edge vortex (“vortex lift”) to the total lift is larger. In this case there is a direct correlation between the wing stall and the occurrence of vortex breakdown on the wing. As discussed earlier, two main parameters could be targeted in order to delay vortex breakdown. These are the swirl level and the external pressure gradient. The latter is easier to control by adding momentum in the axial direction. For this purpose, small aspect ratio jets [44] have been used on the wing surface or above (on fuselage for example) in various applications as sketched in Figure 12. These may be called “along-the-core blowing”.

Figure 12 also shows trailing-edge blowing which has applications to thrust-vectoring and can modify the external pressure gradient. On the other hand, the second parameter, swirl level, can be controlled by leading-edge blowing or suction. It is noted that blowing at the leading-edge may produce an undesired effect and increase the circulation of the leading-edge vortex. However, depending on the direction of blowing, such as blowing inboard using the Coanda effect, leading-edge blowing may add some momentum in the axial direction. Suction is likely to be more effective than blowing as the strength (circulation) of the vortex can be decreased in order to delay vortex breakdown. The effectiveness of along-the-core blowing, trailing-edge blowing and leading-edge suction or blowing is compared in Figure 13. Here the effectiveness is defined as the ratio of the normalized delay in breakdown location to the momentum coefficient [44]. It is seen that along-the-core blowing is the most effective method, whereas trailing-edge blowing is the least effective method.

For nonslender delta wings ($\Lambda \leq 55^\circ$), the contribution of the leading-edge vortex (vortex lift) to the total lift is smaller. Hence, there is no correlation between the vortex breakdown and the wing stall. Instead, the wing stall is directly related to the failure of the reattachment of the flow on the wing surface. As discussed earlier, reattachment on the wing surface can be made possible using well-known separation control methods. Excitation of the shear layer instabilities is known to be the most effective method for separation control [45]. In Figure 14(a), the excitation is produced by small amplitude wing oscillations and the time-averaged vortices are visualized [44]. It is seen that the effect of the excitation is small for pre-stall angles of attack ($\alpha = 15^\circ$) where there is already reattachment for the baseline flow. For near-stall ($\alpha = 20^\circ$) or post-stall angles of attack ($\alpha = 25^\circ$), reattachment occurs inboard of the vortices. The instantaneous images in Figure 14(b) for the largest angle of attack reveal the effect of the excitation on the separated shear layer and the occurrence of small-scale vortices (the dashed line indicates the wing symmetry plane). Yaniktepe and Rockwell [46] showed that small perturbations of wing motion might be effective for an even lower sweep angle of $\Lambda = 38.7^\circ$. The promotion of reattachment and delayed stall by means of small amplitude forced oscillations of the wing can also be achieved with other actuators used for active flow control, such as synthetic jets [30] and pulsed jets [29, 47,48]. An interesting passive control mechanism has been observed for flexible nonslender delta wings [49] where the periodic excitation (wing leading-edge vibrations) is produced as a result of the fluid-structure interaction. In this case there is no need for external power to achieve the delayed stall.

An interesting aspect of the vortex control on nonslender delta wings is illustrated in Figure 15. The effect of excitation with a pulsed jet on the time-averaged flow in a crossflow plane [29] is shown in Figure 15(a). The flow reattachment near the wing symmetry plane with excitation is visible. Whether there is axial flow through the vortices has been debated for this type of vortices. Figure 15(b) reveals that, in a plane through the vortex axis, there is virtually no axial flow. In other words, with flow control, a vortex with breakdown is formed from massively separated flow.

Multiple vortices over delta wings, such as those found on double delta wings, may offer both challenges and potential benefits in terms of flow/vortex control. In Figure 16(a), a three-dimensional view of the time-averaged vorticity for the baseline flow [34] is shown for a $70^\circ/50^\circ$ double delta wing at an angle of attack of $\alpha = 12^\circ$. The wing and strake vortices in the baseline case are well separated although there is an indication of rotation around each other towards the trailing-edge. When blowing is applied at a momentum coefficient of $C_{\mu} = 2\%$ at an upstream location, one gets a variety of vortex topologies, by varying the jet yaw angle for a fixed pitch angle. In Figure 16(b), the baseline case (top) and those for the yaw angle of $\beta = 30^\circ$ (middle) and $\beta = 75^\circ$ (bottom) are shown at $x/c = 0.875$. It is seen that either both vortices are displaced inboard (and remain separated) or merge into a single one, depending on the jet yaw angle. In the case of merging, this is promoted by the ingestion of the jet turbulence into the vortices. Vortex interactions can also be manipulated through passive bleed by exploiting the pressure difference between the upper and lower wing surfaces [34]. In Figure 16(c), for the same wing and measurement station, the effect of the spanwise location of the bleed hole at an upstream station is shown for two different cases (top $y_b/s = 0.10$ and bottom 0.42). It is remarkable that passive bleed with estimated momentum coefficient of the order of 0.1% can also promote vortex merging. For both active jet blowing and passive bleed, significant changes in the vorticity centroid of the vortex system were observed, suggesting that great potential exists to generate forces/moments for flight control.

B. Control of tip vortices of high aspect ratio wings

Diverse objectives ranging from the reduction of induced drag, generation of forces and moments, to diffusing the tip vortices have been considered. As increasing the effective span

decreases the induced drag, spanwise blowing from the wing tip was investigated both experimentally [50] and computationally [51]. Using wing-tip blowing, a reduction in the maximum time-averaged tangential velocity was achieved [52]. The diversity of vortex configurations is immense even for a cut-off (square) wing tip [1] (see the inset in Figure 17). Depending on the direction of continuous blowing, one obtains very different vortex topologies which may be useful for different purposes. The example shown in Figure 17 was obtained by blowing upwards (Slot 1) with a momentum coefficient of 1%. While multiple vortices are evident, the whole vortex system is displaced inboard, revealing its potential for roll control of aircraft. With blowing downwards (not shown here), the vortex system could be displaced outboards, resulting in an increase in the effective span. Significant changes in the circulation of the vortices are also possible, depending on the blowing configuration. When the wing flow is separated in the baseline case (such as schematically shown in Figure 3(a)), significant changes in the location of the tip vortex are possible [53,54] by applying separation control to the wing flow.

When spanwise blowing [1] is applied near the pressure surface (Slot 3 in the inset) with a momentum coefficient of 1%, a highly diffused time-averaged vortex could be obtained as already shown in Figure 7. The vortical flow of the jet, hence turbulence, appears to be ingested rapidly during the formation process of the tip vortex. Some of this substantial diffusion of the time-averaged vortex is due to the increasing meandering with blowing. Although the reduction of the time-averaged vorticity is partly due to the meandering, there is still a reduction in the instantaneous crossflow velocity. This could be useful in some applications as will be discussed later on. Turbulence ingestion into the developing tip vortex can be achieved for much lower momentum coefficients (on the order of 0.1%) with synthetic jets [55].

C. Attenuation of wing-rock

Control of wing-tip vortices during the unsteady motion of the wing can be beneficial. The best known example is the attenuation of wing rock, which is a limit-cycle motion of the wing as a result of the vortex-wing interaction. This motion is not limited to the slender delta wings. In Figure 18(a), the time history of roll angle is shown for a rectangular wing with aspect ratio of two [56]. In the baseline case, large roll angle oscillations reaching 50 degrees are observed at an angle of attack of 17 degrees, which is near the stall angle for the stationary wing. With external acoustic forcing at $St = 1.5$, it is seen that large roll oscillations

have been eliminated. In Figure 18(b), the phase-averaged velocity magnitude is shown over the flat plate wing at zero roll angle (and increasing) at a spanwise location of $y/(b/2) = -0.5$ for the baseline case (left) and with the acoustic forcing (right). It is seen that, with the acoustic forcing, there is reattachment and a large separation bubble in the phase-averaged flow. In Figure 18(c), the crossflow velocity vectors and the magnitude of the standard deviation of the velocity are shown near the trailing-edge at zero roll angle (and increasing) for the baseline case (top) and with the acoustic forcing (bottom). In the baseline case, the asymmetry of the separated flow from the leading-edge of the wing as well as the asymmetry of the tip vortices are apparent. The stronger vortex with larger velocities is closer to the wing surface and drives the wing rotation in the counter-clockwise direction at this phase. With the acoustic forcing, the vortices appear more symmetric at the same phase. In this example, the control of separation from the leading-edge by means of external acoustic forcing is the flow physics behind the attenuation of the wing-rock. In another study, more localized excitation of the shear layer separated from the leading-edge by means of a synthetic jet resulted in similar attenuation of the wing rock [57].

An equally successful, but entirely different method for attenuation of wing rock, exploits the incoherent nature of the tip vortices by means of passive bleed [32]. As discussed earlier, bleed near the wing tip may lead to incoherent and diffused tip vortices as shown in Figure 10. Bleed slot geometries shown in this figure cause substantial attenuation of the wing rock of the rectangular wing with aspect ratio of two. In Figure 19, phase-averaged streamwise vorticity is shown in a crossflow plane at $x/c = 0.5$ at zero roll angle (increasing and decreasing) as well as for the stationary wing for the baseline case (top) and two slot geometries. Note that a spanwise distance of one-eighth of the wing span is shown in the figures. In the baseline case, the tip vortices at the two zero roll angles (increasing and decreasing) are very different from each other, and also from the one for the stationary wing, revealing hysteresis. For slot C (middle row), the jet-like bleed and the resulting interactions between the counter-clockwise vorticity and the shear layer separated from the wing tip as well as between the clockwise vorticity shed from the tip and slot prevent the formation of a coherent vortex. It is seen that the vorticity patterns of the stationary wing and free-to-roll wing are similar, since the roll oscillations were nearly eliminated. For slot D (bottom row), there are again interactions between the regions of clockwise vorticity shed from the tip and the slot, which prevent the formation of the coherent tip vortex observed over the stationary

baseline model. It is interesting that the attenuation of wing rock with passive bleed is successful for all angles of attack, whereas those using active flow control are able to delay the onset of the roll oscillations by up to 4 degrees, but ineffective at larger incidences. This is one of the rare examples where the passive control method is far superior to the active control methods.

D. Attenuation of vortex-wing interaction

Trailing vortices of large aircraft present wake hazard for following aircraft. Two main approaches were taken to attenuate the rolling moment on the wings of the following aircraft due to the trailing vortices [40]. In the first approach, the aim is to excite the instabilities of vortex pairs in order to accelerate the vortex linking, break-up and dissipation of the wake. The excitation of the Crow instability using aircraft's control surfaces [40] and pulsed spanwise blowing at the wing tip [58] have been suggested.

The second approach is to reduce the maximum tangential velocity of the tip vortex in order to attenuate the rolling moment on following aircraft. Turbulence ingestion by means of blowing [1,52] and passive turbulence generators such as small airfoils and spoilers [38,39] are among the methods investigated. Although passive devices did not reveal significant potential for the reduction of vortex-induced rolling moments [59], they may have benefits in the reduction of vortex-induced loads, vibration and noise on helicopter blades [38,39].

Leading-edge vortices can also be a source for unsteady loads and buffeting on downstream wings and fins [60]. In particular, the helical mode instability of vortex breakdown flow field causes quasi-periodic pressure fluctuations on downstream surfaces [13,15]. The delay or elimination of vortex breakdown as well as alteration of the vortex trajectory, for example by means of fences [61], may be beneficial for the attenuation of wing and fin buffeting. However, the success of this type of vortex control is likely to be highly dependent on the angle of attack and roll angle, and possibly on the unsteady maneuvers.

E. Drag reduction of afterbody vortices

This is totally different from other cases in which it is desired to strengthen the vortices in order to increase the lift or moment. Afterbody vortices that are formed on cylindrical bodies with a slanted base (see the example in Figure 20) are the main source of the drag for upsweep angles less than a critical value (which is between 45° and 50°). In fact, it was found

that the strength of the vortices at the trailing-edge was proportional to the time-averaged drag coefficient [3]. In order to achieve drag reduction, one wishes to displace the vortices away from the surface, weaken, diffuse, disintegrate or eliminate the vortices by means of active and passive flow control methods. Mini-spoilers on the upswept surface have been investigated as a potential method to displace and also disintegrate the vortices [62]. Two examples are shown in Figure 20, each with a height-to-diameter ratio of 5% and normal to the surface, located at 2.5% and 87.5% of the distance along the upswept section. The most upstream mini-spoiler does not prevent the formation of the afterbody vortex, but causes it to be very diffused further downstream. The flow in the symmetry plane shown in Figure 20 reveals that the spoiler causes separation, and ingestion of turbulence is likely to be the reason for the diffused vortex. However, this case has the highest drag due to the negative pressures in the separation region just downstream of the spoiler. When the spoiler is moved further downstream, it causes vortex breakdown by creating an adverse pressure gradient in addition to producing turbulence that diffuses the vortex. Again, the total drag may increase due to the spoiler-induced separation on the upswept surface. At a sufficiently downstream location of the spoiler, drag reduction is possible. The best location of the spoiler (87.5% of the distance along the swept section) produces a drag reduction of around 5%. At first glance, Figure 20 suggests that there is little difference in the vorticity field from the baseline case. However, upon close inspection, it has been observed that the vortex is displaced further away from the surface due to the spoiler, which acts like a Gurney flap (see also the flow in the symmetry plane). It is clear that different flow mechanisms, including spoiler-induced separation, turbulence ingestion, and deflection of vortex trajectory are all involved in this case.

Active flow control using continuous blowing has also been investigated for this geometry [63]. It was thought that blowing upstream in the vortex core would be the most effective way to disintegrate the afterbody vortices. This is schematically shown in the inset of Figure 21(a). The streamwise vorticity in the crossflow plane at the trailing-edge is shown for the baseline case and with blowing at a momentum coefficient of 1% per jet (2% total). With flow control, the vortex breaks down and one expects that there would be drag reduction. However, note that there is also negative thrust, which means drag, of the two jets due to their upstream direction. In this case, the total drag increased about 1% due to the combined effect of jet drag and the likely decrease in the vortex drag.

It is possible to achieve vortex-drag reduction with a different flow mechanism while having the positive thrust of the jets. This is illustrated in Figure 21(b). The inset schematically shows blowing from a slot in the direction of the freestream. The streamwise vorticity in two crossflow planes at distances of 20% and 40% of the distance along the upswept section is shown for the baseline case and with blowing at a momentum coefficient of 2%. With blowing, shear layer roll-up occurs more outboard due to the interaction with the jet. The resulting vortices have lower circulation. In this case, drag reduction of about 9% and, more importantly, a net energy savings of almost 3%, have been achieved by this jet flap. It is clear that the roll-up and formation of the afterbody vortices can be effectively controlled.

V. Conclusions

Flow control of tip and edge vortices shed from wings and bodies requires manipulation of their location and structure. The objectives may vary from displacing the vortices closer to or away from the wing surface, displacing them inboard or outboard, increasing their strength, and delaying vortex breakdown, to making them diffused, incoherent and rapidly disintegrated. Consequently, flow control strategies may widely differ. The flow phenomena and main parameters that impact on the vortex structure are briefly reviewed. These include flow separation from the edge/tip, vortex formation, circulation, axial flow, external pressure gradient, wing flow near the edge, vortex breakdown, vortex instabilities, interaction of co- and counter-rotating vortices, and turbulence ingestion into the vortex. It was noted that some of these are coupled, which may or may not be favourable in terms of the objective of vortex control. The simplest example is that stronger vortex is needed for lift enhancement on a delta wing, but this may trigger vortex breakdown, which in turn may cause a decrease in the lift. Further research opportunities remain in the excitation of vortex instabilities, manipulation of multiple vortices, and effective exploitation of turbulence ingestion into the vortices.

Flow control methods and actuators for vortex control have been discussed. These include continuous blowing and suction, unsteady blowing, small aspect ratio jets, bleed, plasma actuators and control surfaces. Most of these actuators add momentum as well as vorticity and turbulence into the flow field. Again, there may be cross-coupling between the effects of the actuators. For example, in the case of blowing, the direction and location of the jet slot/hole may affect both the strength and the axial flow along the vortex axis.

A critical review of various vortex control categories is presented, comparing the effects of various flow mechanisms and actuation methods. These include control of delta wing vortices, control of tip vortices of high aspect ratio wings, attenuation of wing-rock, control of interaction of vortices with downstream surfaces, and control of afterbody vortices. In the case of slender delta wings, it was pointed out that vortex breakdown can be delayed by manipulating the pressure gradient, whereas separation control is unlikely to be successful as the reattachment of the flow on the wing surface will not occur. Well-known separation control techniques are effective for non-slender delta wings. Exploitation of multiple co-rotating vortices and bleed are among the promising methods investigated.

Tip vortices of high aspect ratio wings have been manipulated to increase the effective span, to generate rolling moment, to alter the wing loading, or to decrease the tangential velocity. Turbulence ingestion by blowing and manipulation of the tip vortex by means of forced reattachment of the flow on the wing surface are among the most effective applications. Separation control of wing flow and bleed near the wing tip are effective for the attenuation of wing-rock induced by the tip vortices. Altering the trajectory and diffusing the vortex might be effective for vortex-rotorcraft blade interaction and fin buffeting. However, it is not clear whether this approach can be effective in the far-wake of large aircraft. Excitation of the Crow instability may offer a better alternative in this case.

The drag reduction of afterbody vortices is possible by means of active and passive flow control. The latter is achieved by placing a mini-spoiler near the trailing-edge, which acts like a Gurney flap and deflects the vortices away from the surface. The active flow control by blowing was demonstrated to interfere with the roll-up process, resulting in a drag reduction of about 9% and a net energy savings of about 3%.

Acknowledgements

This review article has been written while the authors were supported by a grant from the Air Force Office of Scientific Research, Air Force Material Command, USAF, under Grant Number FA9550-14-1-0126, on the control of afterbody vortices. The authors acknowledge

previous financial support by the Air Force Office of Scientific Research (AFOSR), Engineering and Physical Sciences Research Council (EPSRC), the Ministry of Defence in the UK, and the EC 6th Framework Programme, which led to the work reviewed here.

References

- [1] Margaris, P., and Gursul, I., “Vortex Topology of Wing Tip Blowing”, *Aerospace Science and Technology*, Vol. 14, No. 3, 2010, pp. 143-160. [doi:10.1016/j.ast.2009.11.008](https://doi.org/10.1016/j.ast.2009.11.008)
- [2] Ma, B.-F., Wang, Z., and Gursul, I., “Symmetry Breaking and Instabilities of Conical Vortex Pairs over Slender Delta Wings”, *Journal of Fluid Mechanics*, vol. 832, 2017, pp. 41-72. [doi:10.1017/jfm.2017.648](https://doi.org/10.1017/jfm.2017.648)
- [3] Bulathsinghala, D., Jackson, R., Wang, Z., and Gursul, I., “Afterbody Vortices of Axisymmetric Cylinders with a Slanted Base”, *Experiments in Fluids*, 58:60, 2017. [doi:10.1007/s00348-017-2343-9](https://doi.org/10.1007/s00348-017-2343-9)
- [4] Gad-el-Hak, M., and Blackwelder, R. F., “The Discrete Vortices from a Delta Wing”, *AIAA Journal*, Vol. 23, 1985, pp. 961-962. [doi:10.2514/3.9016](https://doi.org/10.2514/3.9016)
- [5] Gordnier, R., and Visbal, M. R., “Unsteady Vortex Structure over a Delta Wing”, *Journal of Aircraft*, Vol. 31, 1994, pp. 243-248. [doi:10.2514/3.46480](https://doi.org/10.2514/3.46480)
- [6] Cipolla, K. M., and Rockwell, D., “Small-Scale Vortical Structures in Crossflow Plane of a Rolling Delta Wing”, *AIAA Journal*, Vol. 36, 1998, pp. 2276-2278. [doi:10.2514/2.338](https://doi.org/10.2514/2.338)
- [7] Batchelor, G.K., "Axial Flow in Trailing Line Vortices", *Journal of Fluid Mechanics*, Vol. 20, No. 4, 1964, pp 645-658. [doi:10.1017/s0022112064001446](https://doi.org/10.1017/s0022112064001446)
- [8] Hall, M.G., “Vortex Breakdown”, *Annual Review of Fluid Mechanics*, Vol. 4, 1972, pp. 195-218. [doi:10.1146/annurev.fl.04.010172.001211](https://doi.org/10.1146/annurev.fl.04.010172.001211)

- [9] Hall, M.G., “A Theory for the Core of a Leading-Edge Vortex”, *Journal of Fluid Mechanics*, Vol. 11, 1961, pp. 209- 228. doi:10.1017/s0022112061000470
- [10] Leibovich, S. “Vortex Stability and Breakdown: Survey and Extension”, *AIAA Journal*, vol. 22, 1984, pp. 1192-1206. doi:10.2514/3.8761
- [11] Delery, J. M., “Aspects of Vortex Breakdown,” *Progress in Aerospace Sciences*, Vol. 30, 1994, pp. 1–59. doi:10.1016/0376-0421(94)90002-7
- [12] Escudier, M., “Vortex Breakdown: Observations and Explanations,” *Progress in Aerospace Sciences*, Vol. 25, 1998, pp. 189–229. doi:10.1016/0376-0421(88)90007-3
- [13] Gursul, I., “Review of Unsteady Vortex Flows over Slender Delta Wings”, *Journal of Aircraft*, Vol. 42, 2005, pp. 299-319. doi:10.2514/1.5269
- [14] Parmenter, K., and Rockwell, D., “Transient Response of Leading-Edge Vortices to Localized Suction,” *AIAA Journal*, Vol. 28, No. 6, 1990, pp. 1131–1133. doi:10.2514/3.25177
- [15] Gursul, I., “Unsteady Flow Phenomena over Delta Wings at High Angle of Attack”, *AIAA Journal*, Vol. 32, 1994, pp. 225-231. doi:10.2514/3.11976
- [16] Gursul, I., “Effect of Nonaxisymmetric Forcing on a Swirling Jet with Vortex Breakdown”, *Journal of Fluids Engineering*, Vol. 118, 1996, pp. 316-321. doi:10.1115/1.2817379
- [17] Chen, C., Wang, Z., Cleaver, D.J., and Gursul, I., “Interaction of Trailing Vortices with Downstream Wings”, *AIAA Science and Technology Forum and Exposition (SciTech 2016)*, San Diego, California, United States, 4–8 January 2016, AIAA-2016-1848. doi:10.2514/6.2016-1848
- [18] Leweke, T., Le Dizés, S., and Williamson, C. H. K., “Dynamics and Instabilities of Vortex Pairs”, *Annual Review of Fluid Mechanics*, Vol. 48, 2016, pp. 507-541. doi:10.1146/annurev-fluid-122414-034558

- [19] Tobak, M., and Peake, D.J., "Topology of Three-Dimensional Separated Flows", *Annual Review of Fluid Mechanics*, Vol. 14, 1982, pp. 61-85. [doi:10.1146/annurev.fl.14.010182.000425](https://doi.org/10.1146/annurev.fl.14.010182.000425)
- [20] Keener, E.R., and Chapman, G.T., "Similarity in Vortex Asymmetries over Slender Bodies and Wings", *AIAA Journal*, Vol. 15, 1977, pp. 1370-1372. [doi:10.2514/3.60795](https://doi.org/10.2514/3.60795)
- [21] Degani, D., "Effect of Geometrical Disturbances on Vortex Asymmetry", *AIAA Journal*, Vol. 29, 1991, pp. 560-566. [doi:10.2514/3.59929](https://doi.org/10.2514/3.59929)
- [22] Degani, D., and Tobak, M., "Experimental Study of Controlled Tip Disturbance Effect on Flow Asymmetry", *Physics of Fluids*, Vol. 4, 1992, pp. 2825-2832. [doi:10.1063/1.858338](https://doi.org/10.1063/1.858338)
- [23] Marles, D., and Gursul, I., "Effect of an Axial Jet on Vortex Merging", *Physics of Fluids*, Vol. 20, No. 4, 2008, Article 047101. [doi: 10.1063/1.2907210](https://doi.org/10.1063/1.2907210)
- [24] Margaris, P., Marles, D., and Gursul, I., "Experiments on Jet/Vortex Interaction", *Experiments in Fluids*, Vol. 44, No. 2, 2008, pp. 261-278. [doi:10.1007/s00348-007-0399-7](https://doi.org/10.1007/s00348-007-0399-7)
- [25] Phillips, W.R.C., and Graham, J.A.H., "Reynolds-Stress Measurements in a Turbulent Trailing Vortex", *Journal of Fluid Mechanics*, Vol. 147, 1984, pp. 353-371. [doi:10.1017/s0022112084002123](https://doi.org/10.1017/s0022112084002123)
- [26] Paoli, R., Laporte, F., Cuenot, B., and Poinso, T., "Dynamics and Mixing in Jet/Vortex Interactions," *Physics of Fluids*, Vol. 15, No. 7, 2003, pp 1843-1860. [doi:10.1063/1.1575232](https://doi.org/10.1063/1.1575232)
- [27] McCormick, S., and Gursul, I., "Effect of Shear Layer Control on Leading Edge Vortices", *Journal of Aircraft*, Vol. 33, No. 6, 1996, pp. 1087-1093. [doi:10.2514/3.47061](https://doi.org/10.2514/3.47061)

- [28] Gu, W., Robinson, O., and Rockwell, D., “Control of Vortices on a Delta Wing by Leading-Edge Injection,” *AIAA Journal*, Vol. 31, No. 7, 1993, pp. 1177–1186. doi:10.2514/3.11749
- [29] Williams, N., Wang, Z., and Gursul, I., “Active Flow Control on a Nonslender Delta Wing”, *Journal of Aircraft*, Vol. 45, No. 6, 2008, pp. 2100-2110. doi:10.2514/1.37486
- [30] Margalit, S., Greenblatt, D., Seifert, A., and Wygnanski, I., “Delta Wing Stall and Roll Control Using Segmented Piezoelectric Fluidic Actuators”, *Journal of Aircraft*, Vol. 42, No. 3, 2005, pp. 698-709. doi:10.2514/1.6904
- [31] Milanovic, I.M., and Zaman, K.B.M.Q., “Fluid Dynamics of Highly Pitched and Yawed Jets in Crossflow”, *AIAA Journal*, Vol. 42, No. 5, 2004, pp. 874-882. doi:10.2514/1.2924
- [32] Hu, T., Wang, Z., and Gursul, I., “Passive Control of Roll Oscillations of Low-Aspect-Ratio Wings Using Bleed”, *Experiments in Fluids*, Vol. 55, No. 6, 2014, 1752. doi: 10.1007/s00348-014-1752-2
- [33] Çelik, A., Çetin, C. and Yavuz, M.M. “Effect of Passive Bleeding on Flow Structure over a Nonslender Delta Wing”, *AIAA Journal*, Vol. 55, No. 8, August 2017, pp. 2555-2565. doi:10.2514/1.j055776
- [34] Zhang, X., Wang, Z., and Gursul, I., “Control of Multiple Vortices over a Double Delta Wing”, *AIAA Aviation and Aeronautics Forum and Exposition (AIAA Aviation 2017)*, Denver, Colorado, United States, 5–9 June 2017, AIAA-2017-4122. doi:10.2514/6.2017-4122
- [35] Visbal, M.R., and Gaitonde, D.V., “Control of Vortical Flows Using Simulated Plasma Actuators”, *44th AIAA Aerospace Sciences Meeting and Exhibit*, 9-12 January 2006, Reno, NV, AIAA-2006-0505. doi:10.2514/6.2006-505

- [36] Nelson, R.C., Corke, T.C., He, C., Othman, H., and Matsuno, T., “Modification of the Flow Structure over a UAV Wing for Roll Control”, *45th AIAA Aerospace Sciences Meeting and Exhibit*, 8-11 January 2007, Reno, NV, AIAA-2007-884. [doi:10.2514/6.2007-884](https://doi.org/10.2514/6.2007-884)
- [37] Kroo, I., “Drag Due to Lift: Concepts for Prediction and Reduction”, *Annual Review of Fluid Mechanics*, Vol. 33, 2001, pp. 587-617. [doi:10.1146/annurev.fluid.33.1.587](https://doi.org/10.1146/annurev.fluid.33.1.587)
- [38] McAlister, K.W., Tung, C., and Heineck, J.T., “Devices that Alter the Tip Vortex of a Rotor”, Technical Report NASA/TM-2001-209625, 2001.
- [39] Liu, Z., Russell, J.W., Sankar, L., and Hassan, A.A., “A Study of Rotor Tip Structure Alteration Techniques”, *Journal of Aircraft*, Vol. 38, No. 3, 2001, pp. 473-477. [doi:10.2514/2.2786](https://doi.org/10.2514/2.2786)
- [40] Spalart, P. W., “Airplane Trailing Vortices”, *Annual Review of Fluid Mechanics*, Vol. 30, 1998, pp. 107-138. [doi:10.1146/annurev.fluid.30.1.107](https://doi.org/10.1146/annurev.fluid.30.1.107)
- [41] Deng, Q., and Gursul, I., “Vortex Breakdown over a Delta Wing with Oscillating Leading-Edge Flaps”, *Experiments in Fluids*, Vol. 23, 1997, pp. 347-352. [doi:10.1007/s003480050121](https://doi.org/10.1007/s003480050121)
- [42] Lee, G.B., Shih, C., Tai, Y.C., Tsao, T., Liu, C., Huang, A., and Ho, C.M., “Robust Vortex Control of a Delta Wing by Distributed Microelectromechanical-Systems Actuators”, *Journal of Aircraft*, Vol. 37, No. 4, 2000, pp. 697-706. [doi:10.2514/2.2655](https://doi.org/10.2514/2.2655)
- [43] Mitchell, A.M., and Delery, J., “Research into Vortex Breakdown Control”, *Progress in Aerospace Sciences*, vol. 37, 2001, pp. 385–418. [doi:10.1016/s0376-0421\(01\)00010-0](https://doi.org/10.1016/s0376-0421(01)00010-0)
- [44] Gursul, I., Wang, Z., and Vardaki, E., “Review of Flow Control Mechanisms of Leading-Edge Vortices”, *Progress in Aerospace Sciences*, Vol. 43, 2007, pp. 246-270. [doi:10.1016/j.paerosci.2007.08.001](https://doi.org/10.1016/j.paerosci.2007.08.001)

- [45] Seifert, A., Bachar, T., Koss, D., Shepshelovich, M., and Wygnanski, I., “Oscillatory Blowing: A Tool to Delay Boundary-Layer Separation”, *AIAA Journal*, Vol. 31, No. 11, 1993, pp. 2052-2060. doi:10.2514/3.49121
- [46] Yaniktepe, B. and Rockwell, D. “Flow Structure on a Delta Wing of Low Sweep Angle”, *AIAA Journal*, vol. 42, 2004, pp. 513–523. doi:10.2514/1.1207
- [47] Kölzsch, A. and Breitsamter, C., “Vortex-Flow Manipulation on a Generic Delta-Wing Configuration”, *Journal of Aircraft*, Vol. 51, No. 5, September–October 2014, pp. 1380-1390. doi:10.2514/1.c032231
- [48] Çetin, C., Çelik, A. and Yavuz, M.M., “Control of Flow Structure over a Nonslender Delta Wing Using Periodic Blowing”, *AIAA Journal*, 2017, DOI: 10.2514/1.J056099
- [49] Taylor, G., Wang, Z., Vardaki, E., and Gursul, I., “Lift Enhancement over Flexible Nonslender Delta Wings”, *AIAA Journal*, Vol. 45, No. 12, 2007, pp. 2979-2993. doi:10.2514/1.31308
- [50] Lee, C.S., Tavella, D., Wood, N.J., and Roberts, L., “Flow Structure and Scaling Laws in Lateral Wing-Tip Blowing”, *AIAA Journal*, Vol. 27, No. 8, 1989, pp. 1002-1007. doi:10.2514/3.10211
- [51] Mineck, R.E., “Study of the Potential Aerodynamic Benefits From Spanwise Blowing at Wingtip”, NASA TP-3515, 1995.
- [52] Simpson, R.G., Ahmed, N.A., and Archer, R.D., “Near Field Study of Vortex Attenuation Using Wing-Tip Blowing”, *The Aeronautical Journal*, Vol. 106, Issue 1057, 2002, pp. 117-120. doi:10.1017/S0001924000012847
- [53] Greenblatt, D., “Fluidic Control of a Wing Tip Vortex”, *AIAA Journal*, Vol. 50, No. 2, 2012, pp. 375-386. doi:10.2514/1.j051123
- [54] Greenblatt, D., “Managing Flap Vortices via Separation Control”, *AIAA Journal*, Vol. 44, No. 11, 2006, pp. 2755-2764. doi:10.2514/1.19664

- [55] Margaris, P., and Gursul, I., “Wing Tip Vortex Control Using Synthetic Jets”, *The Aeronautical Journal*, Vol. 110, Issue 1112, 2006, pp. 673-683.
[doi:10.1017/s0001924000001536](https://doi.org/10.1017/s0001924000001536)
- [56] Hu, T., Wang, Z., and Gursul, I., “Attenuation of Self-Excited Roll Oscillations of Low-Aspect-Ratio Wings by means of Acoustic Forcing”, *AIAA Journal*, Vol. 52, issue 4, 2014, pp. 843-854.
doi: 10.2514/1.J052689
- [57] Hu, T., Wang, Z., Gursul, I., and Bowen, C.R., “Active Control of Self-Induced Roll Oscillations of a Wing Using Synthetic Jet”, *International Journal of Flow Control*, Vol. 5, Issue 3-4, 2013, pp. 201-214. [doi:10.1260/1756-8250.5.3-4.201](https://doi.org/10.1260/1756-8250.5.3-4.201)
- [58] Bearman, P., Heyes, A., Lear, C., and Smith, D., “Natural and Forced Evolution of a Counter Rotating Vortex Pair”, *Experiments in Fluids*, Vol. 40, 2006, pp. 98-105.
[doi:10.1007/s00348-005-0051-3](https://doi.org/10.1007/s00348-005-0051-3)
- [59] Dunham, R.E., “Unsuccessful Concepts for Aircraft Wake Minimization”, *Proceedings of the Wake Vortex Minimization Symposium*, NASA SP-409, 1977, pp. 221-250.
- [60] Mabey, D.G., “Some Aspects of Aircraft Dynamic Loads due to Flow Separation”, *Progress in Aerospace Sciences*, Vol. 26, Issue 2, 1989, pp. 115-151.
[doi:10.1016/0376-0421\(89\)90006-7](https://doi.org/10.1016/0376-0421(89)90006-7)
- [61] Shah, G.H., “Wind Tunnel Investigation of Aerodynamic and Tail Buffet Characteristics of Leading-Edge Extension Modifications to the F/A-18”, *AIAA Atmospheric Flight Mechanics Conference*, New Orleans, LA, 12-14 August 1991, AIAA-91-2889. [doi:10.2514/6.1991-2889](https://doi.org/10.2514/6.1991-2889)
- [62] Bulathsinghala, D., Wang, Z., and Gursul, I., “Mini-Spoilers for Afterbody Base Drag Reduction”, *AIAA Aviation and Aeronautics Forum and Exposition (AIAA Aviation*

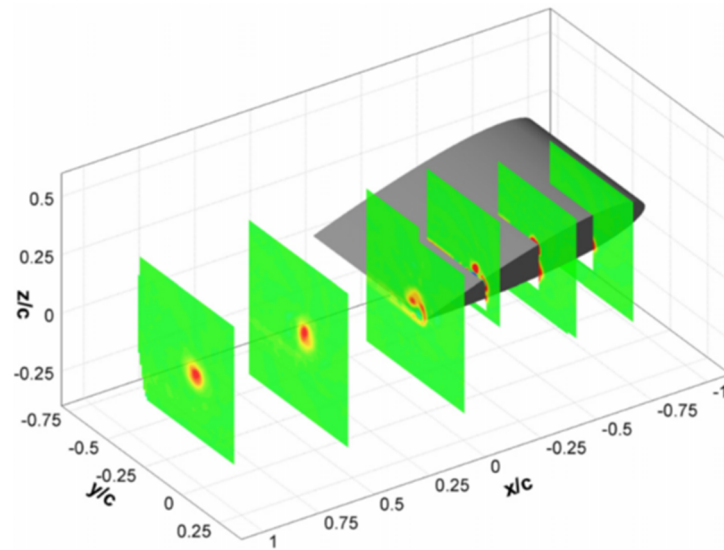
2017), Denver, Colorado, United States, 5–9 June 2017, AIAA 2017-4121.

[doi:10.2514/6.2017-4121](https://doi.org/10.2514/6.2017-4121)

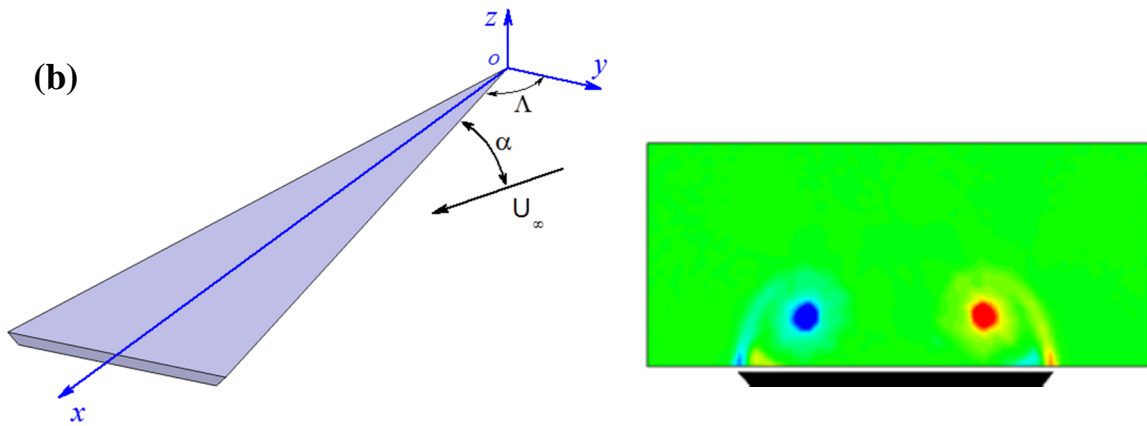
- [63] Jackson, R., Wang, Z., Gursul, I., “Afterbody Drag Reduction Using Active Flow Control”, *AIAA Science and Technology Forum and Exposition (SciTech 2017)*, Grapevine, Texas, United States, 9–13 January 2017, AIAA-2017-0954.

[doi:10.2514/6.2017-0954](https://doi.org/10.2514/6.2017-0954)

(a)



(b)



(c)

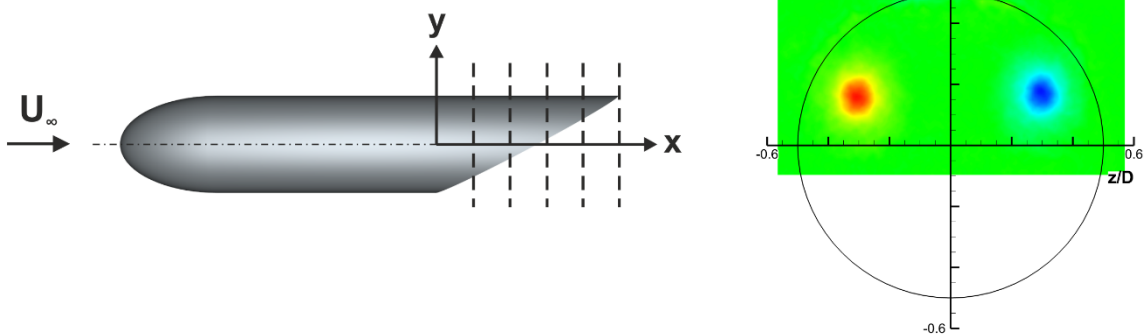
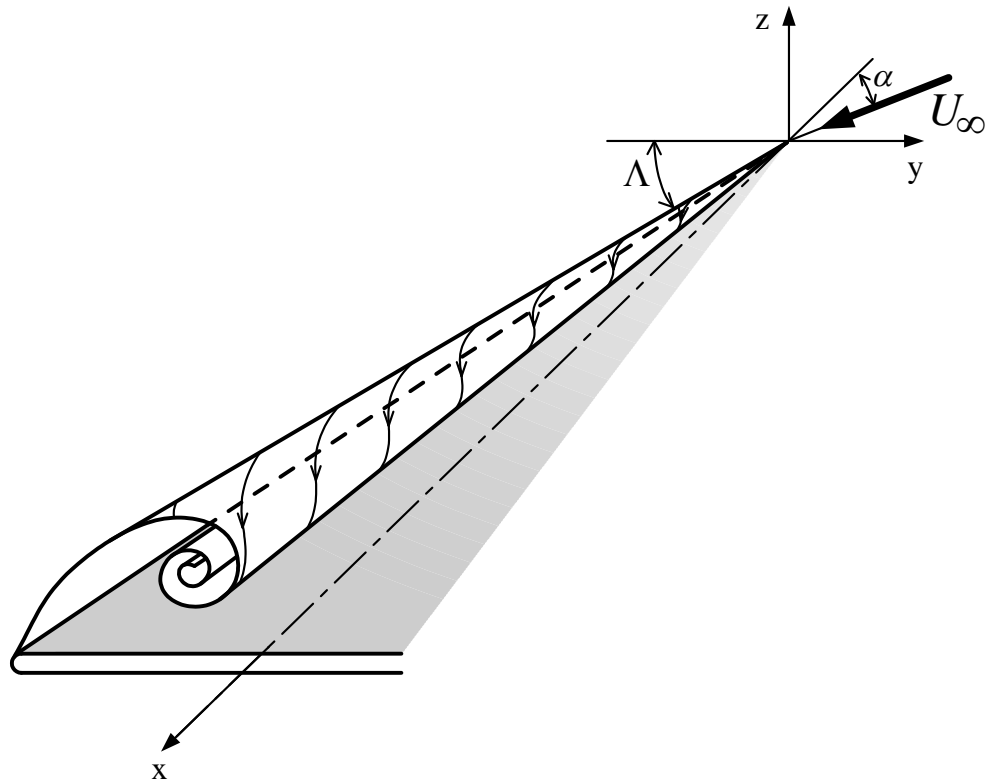


Figure 1: (a) Tip vortex [1]; (b) leading-edge vortices over a delta wing [2]; (c) afterbody vortices [3].

(a)



(b)

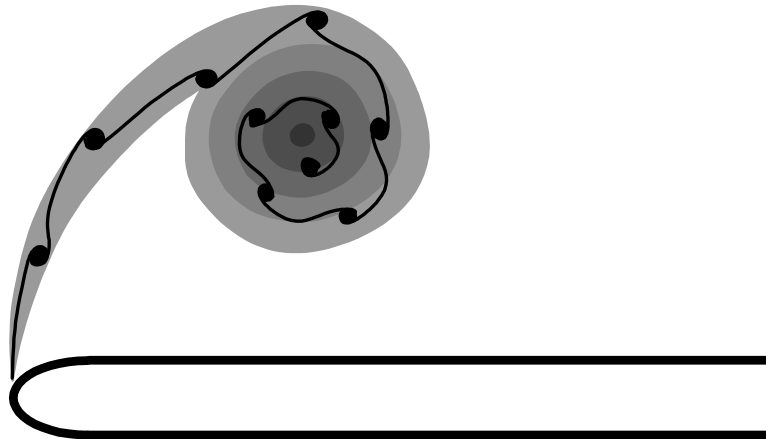


Figure 2: (a) Vortex roll-up; (b) shear-layer instabilities.

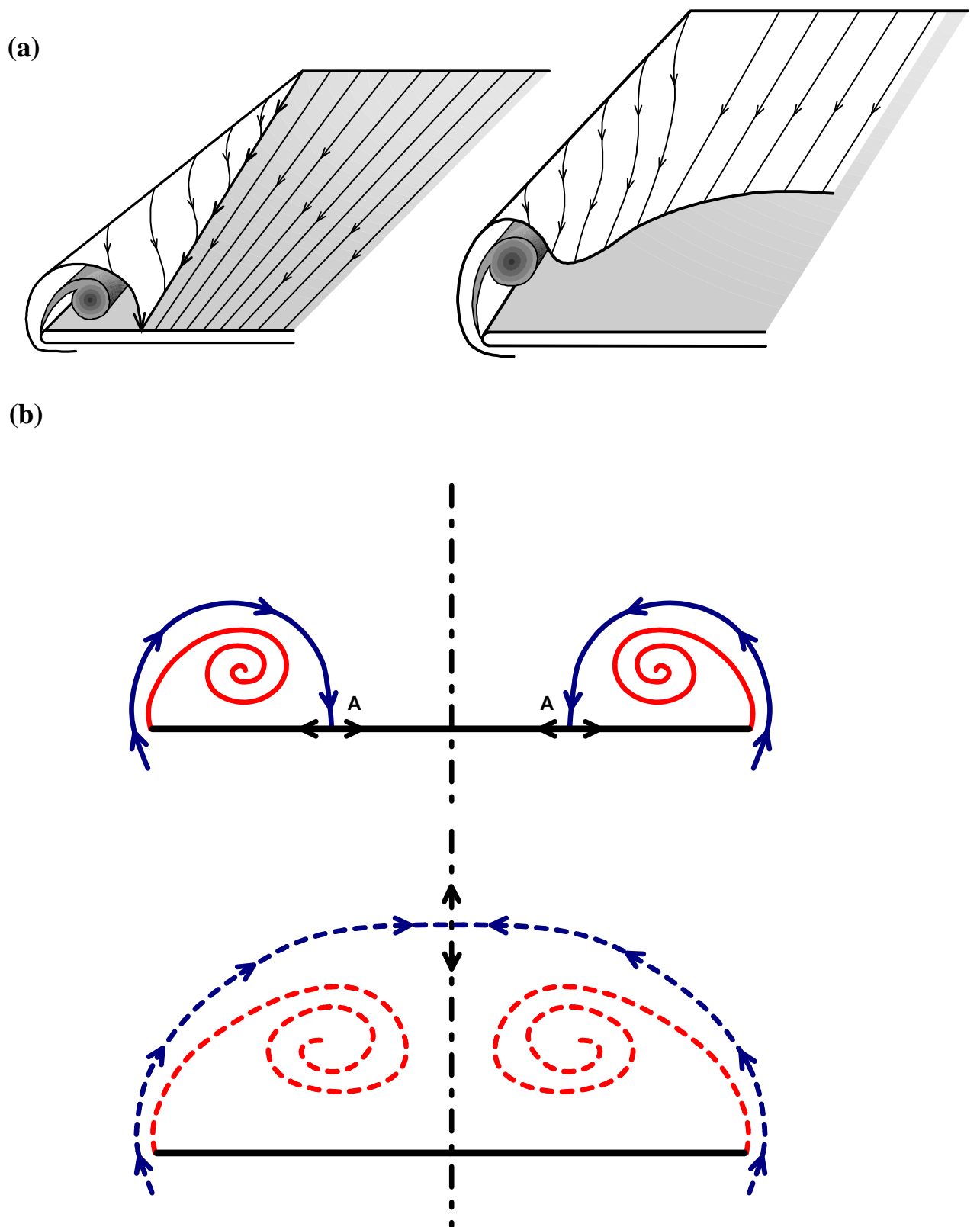


Figure 3: (a) Tip vortices at small and large angles of attack; (b) delta wing vortices at small and large angles of attack.

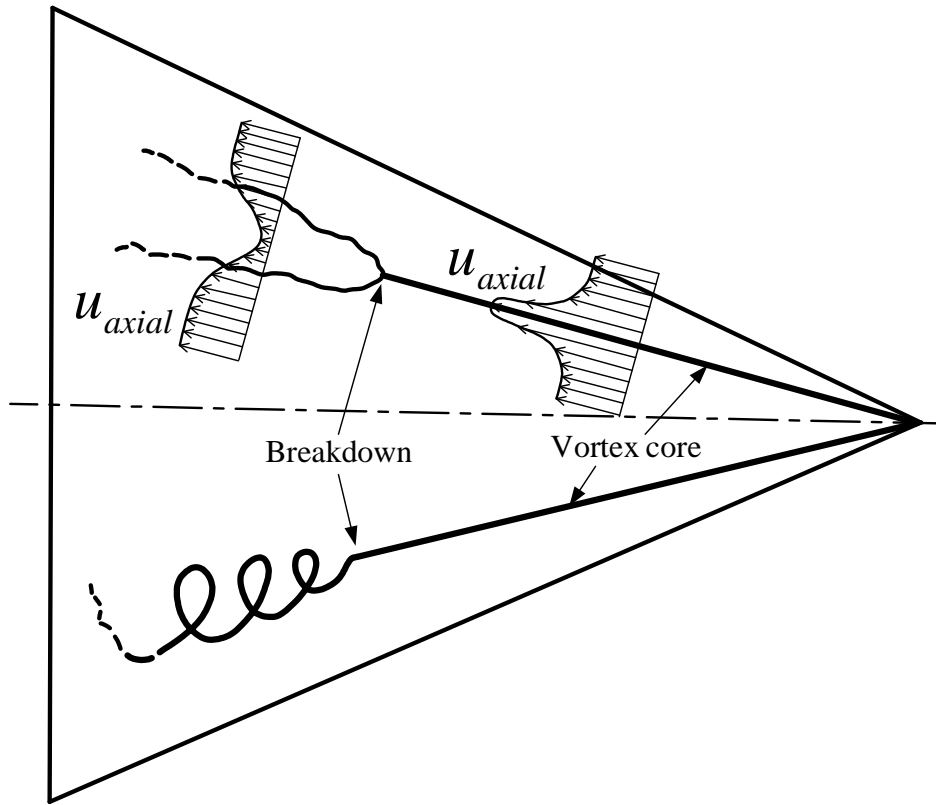
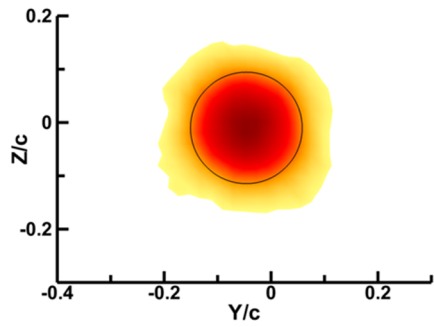


Figure 4 : Bubble and spiral types of vortex breakdown over a delta wing.

Mean vorticity



First POD mode

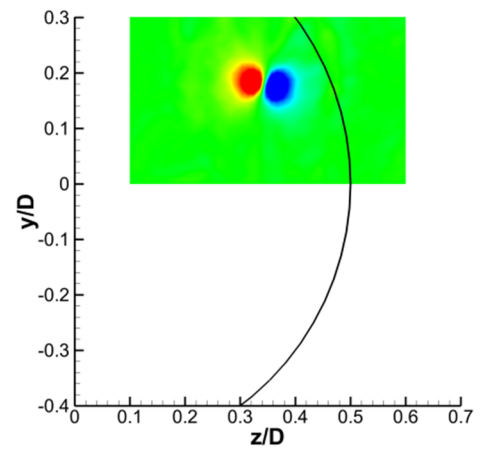
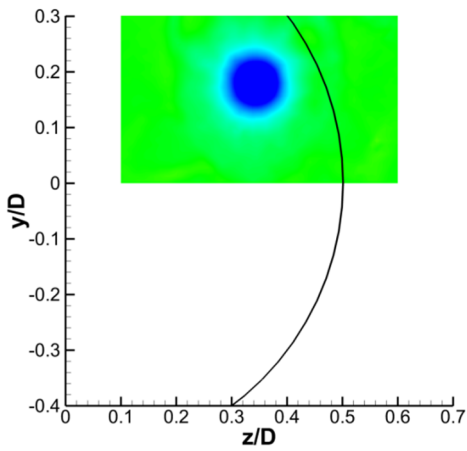
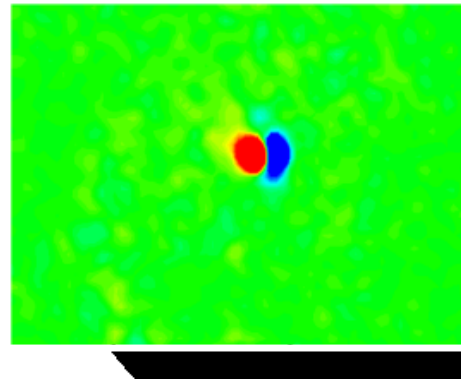
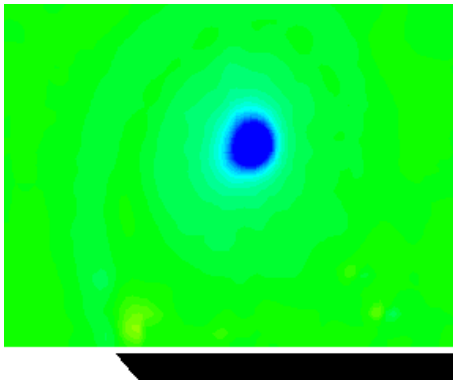
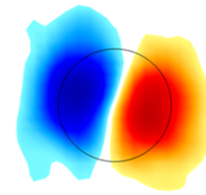
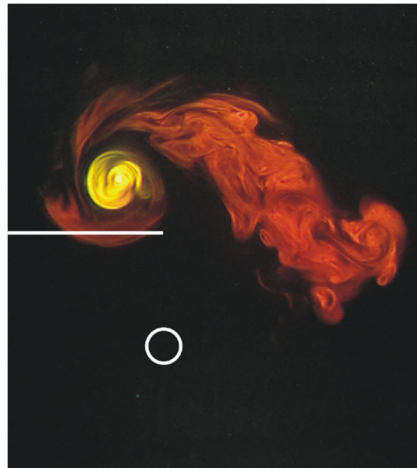


Figure 5: Time-averaged vorticity (left column) and the first POD mode (right column) for a tip vortex [17] (top), delta wing vortex [2] (middle), and afterbody vortex [3] (bottom).

(a)



(b)

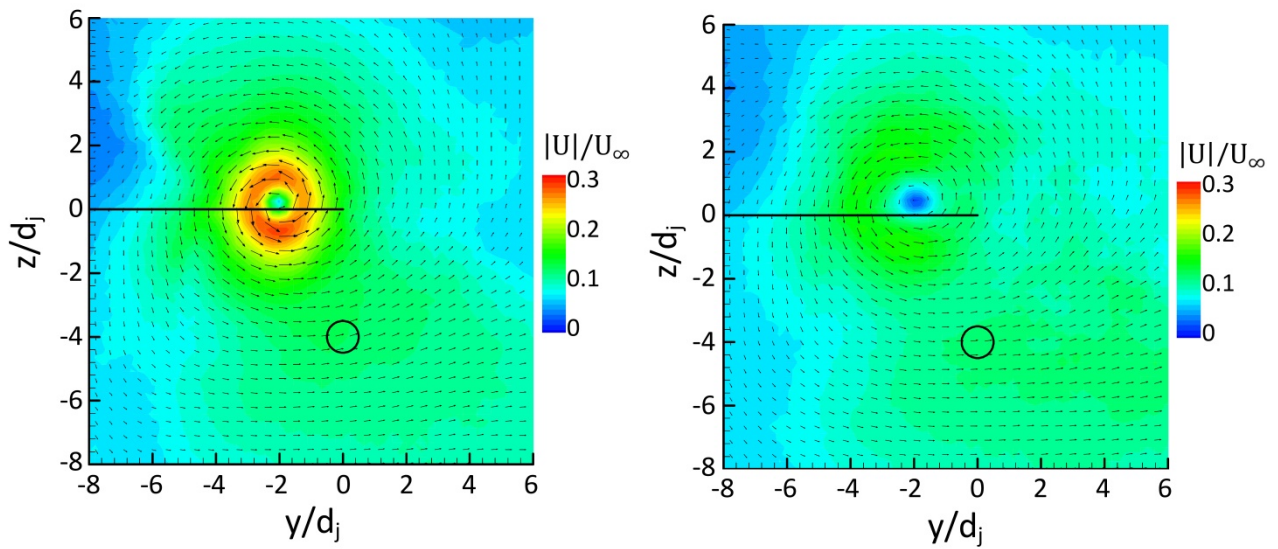


Figure 6: (a) Jet turbulence ingestion into vortex; (b) time-averaged crossflow velocity for the baseline case (left) and with blowing (right) [24].

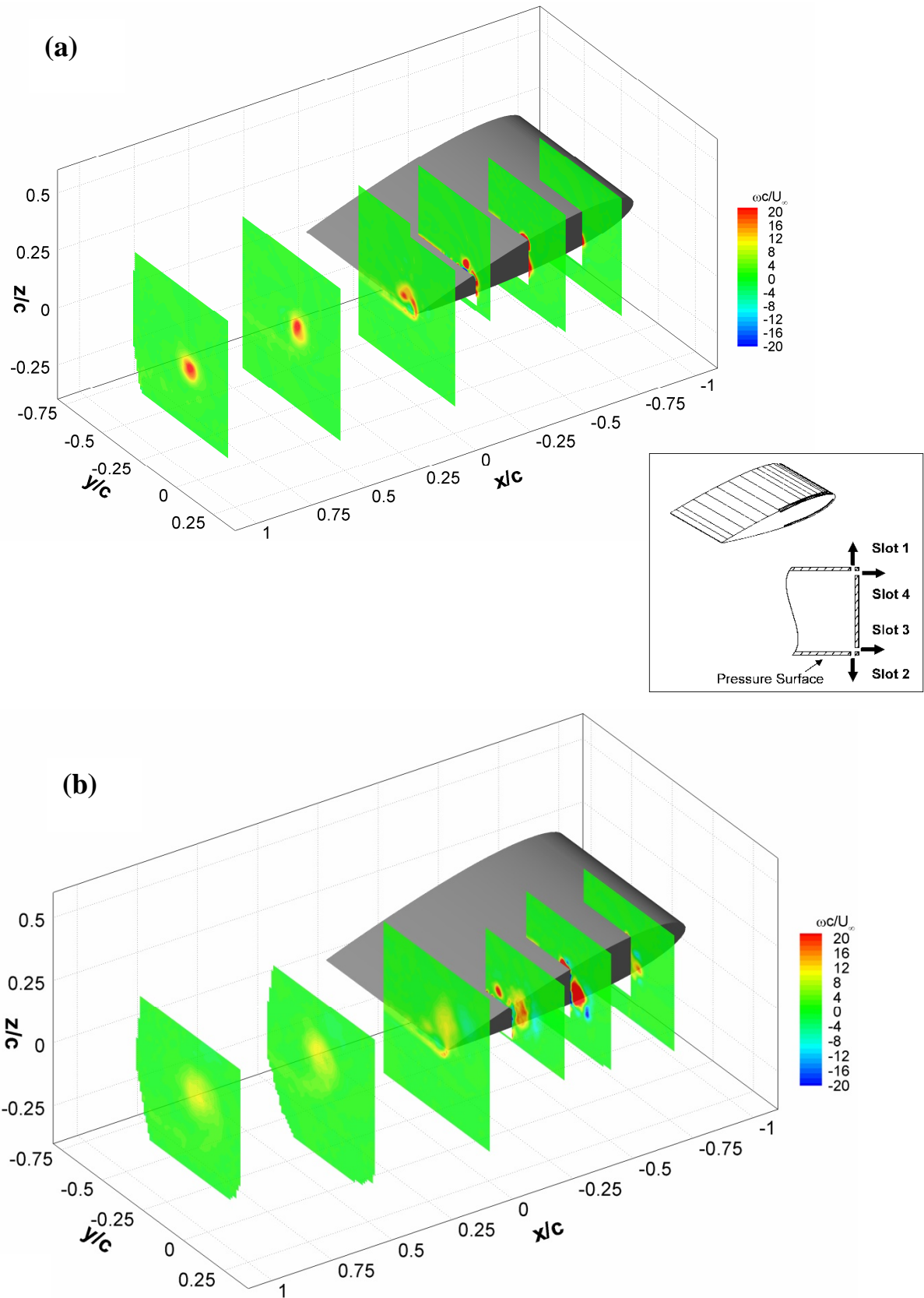


Figure 7: Time-averaged vorticity of (a) baseline tip vortex, (b) with blowing from Slot 3 [1].

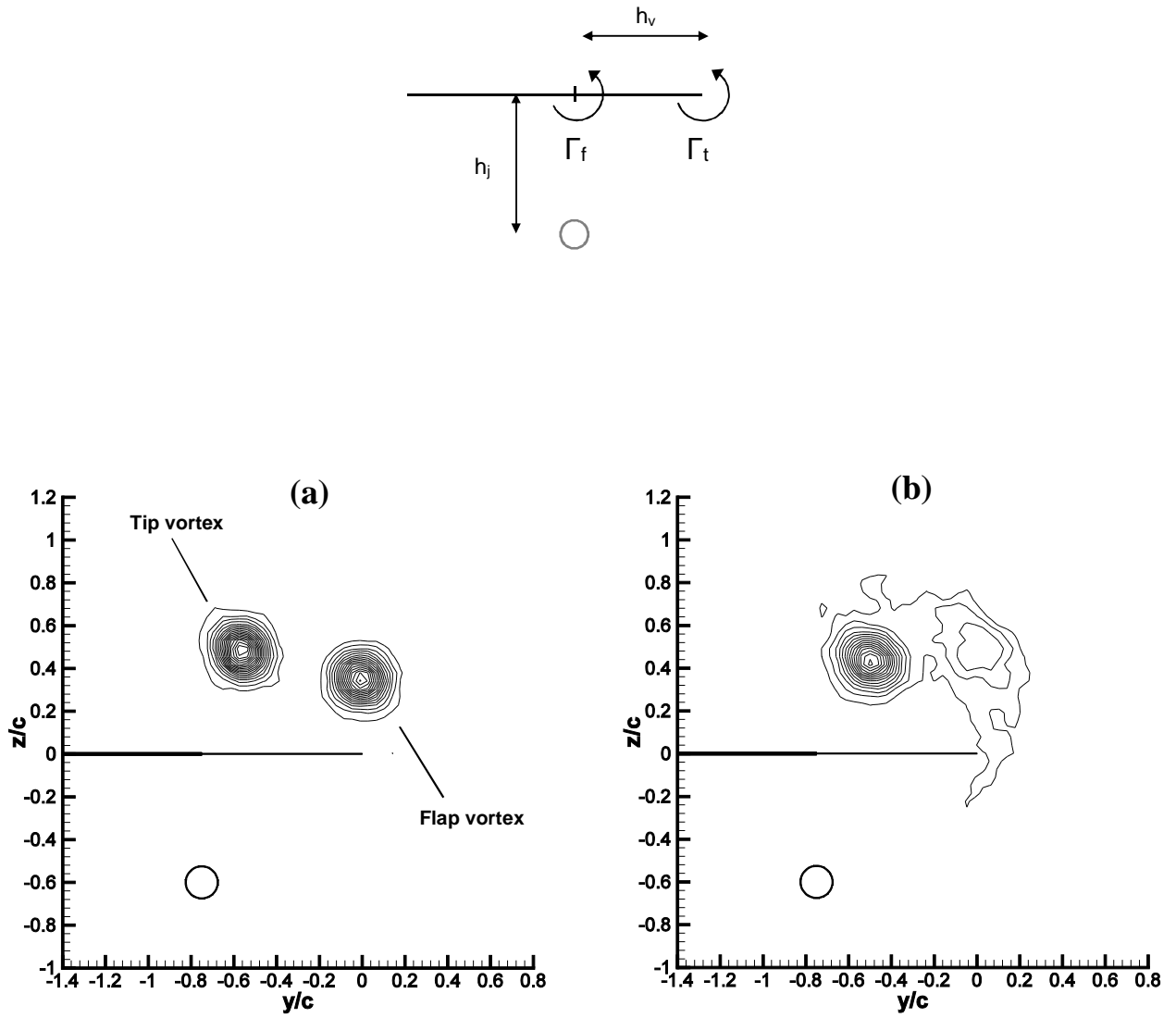
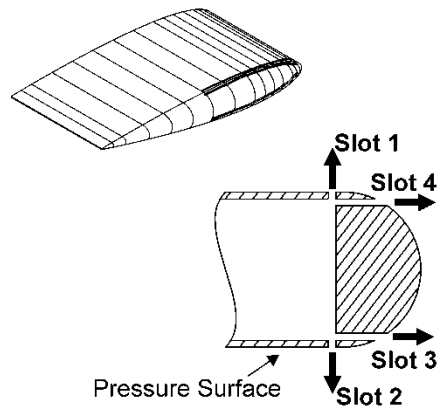


Figure 8: Vorticity contours for (a) baseline case, (b) with blowing [23].

(a)



(b)

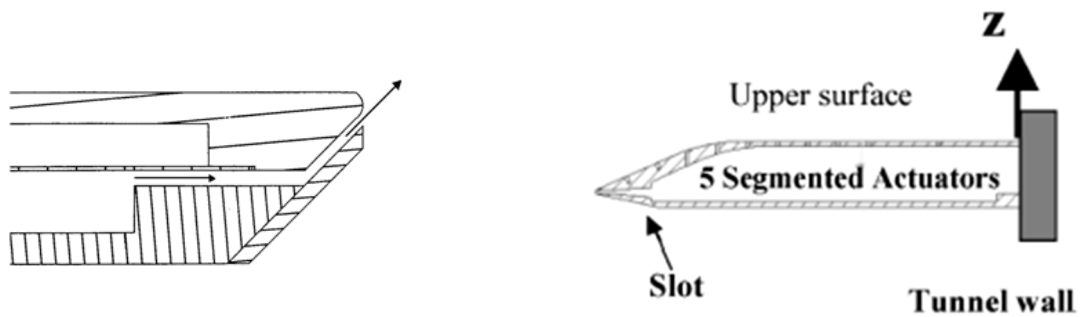


Figure 9: Tip slot geometries for (a) continuous blowing on a rectangular wing [1]; (b) unsteady blowing on nonslender delta wings [29, 30].

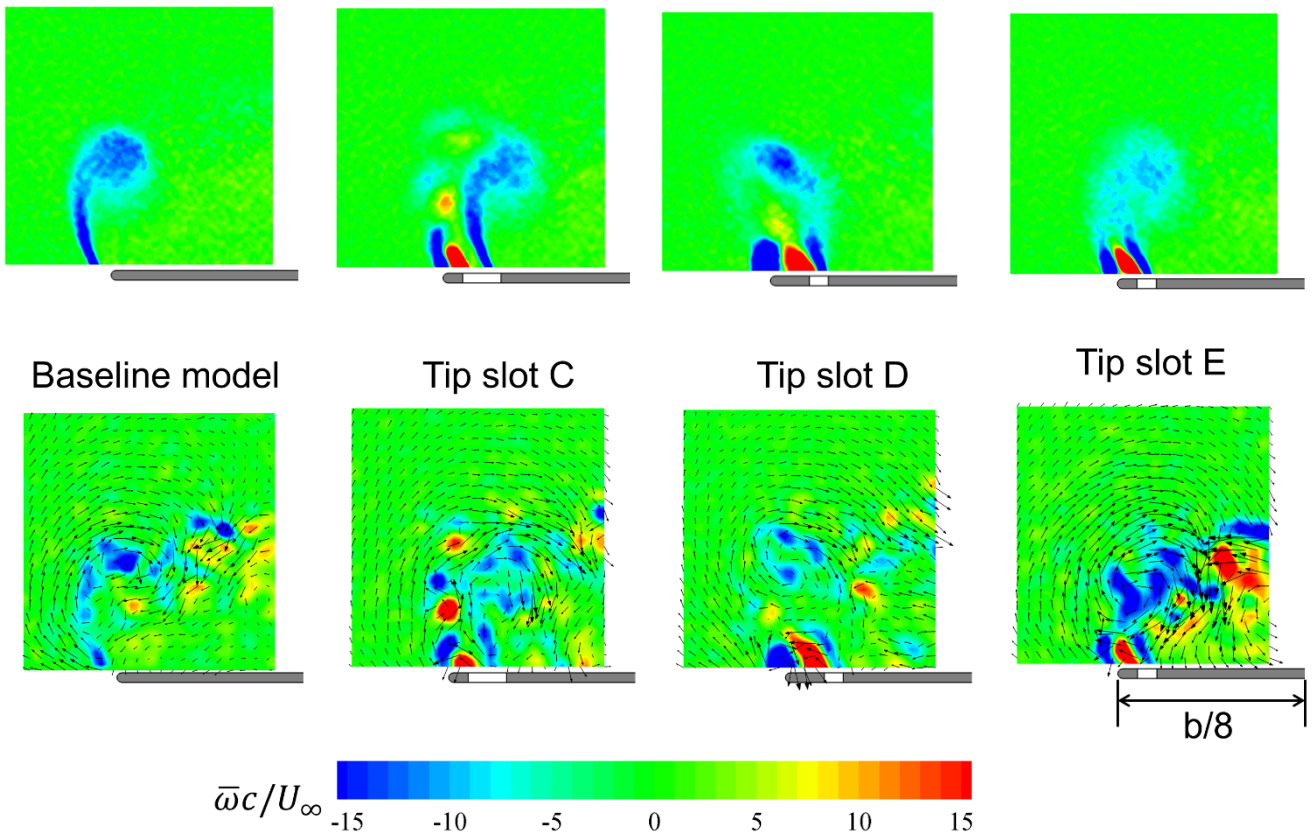
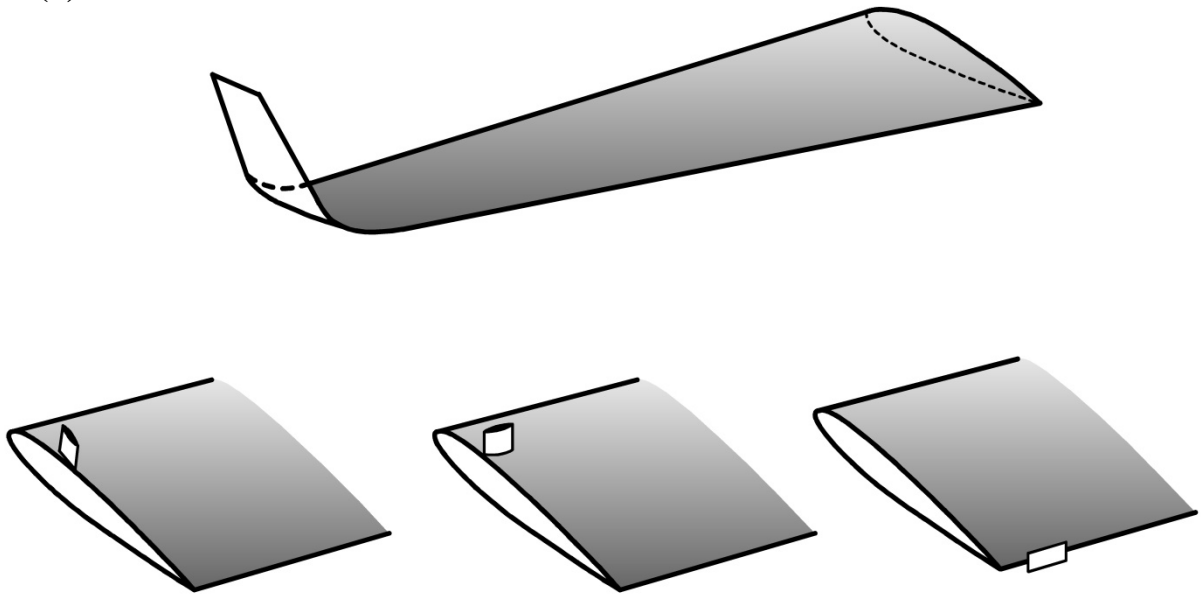


Figure 10: Time-averaged (top) and instantaneous (bottom) vorticity for the baseline wing tip and with various bleed slots [32].

(a)



(b)

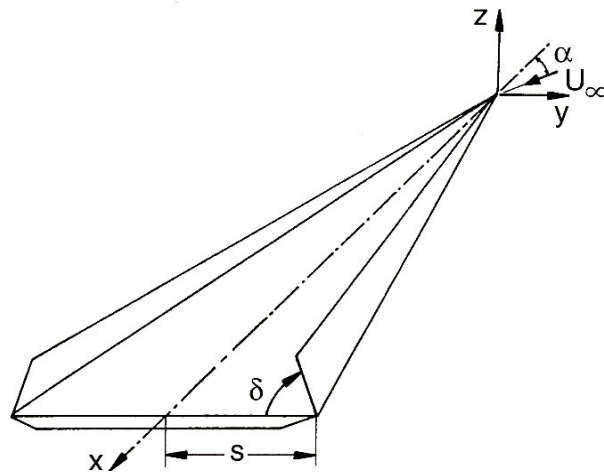


Figure 11: Schematic of (a) winglet and various turbulence generators (adapted from [38,39]), (b) oscillating leading-edge flaps [41].

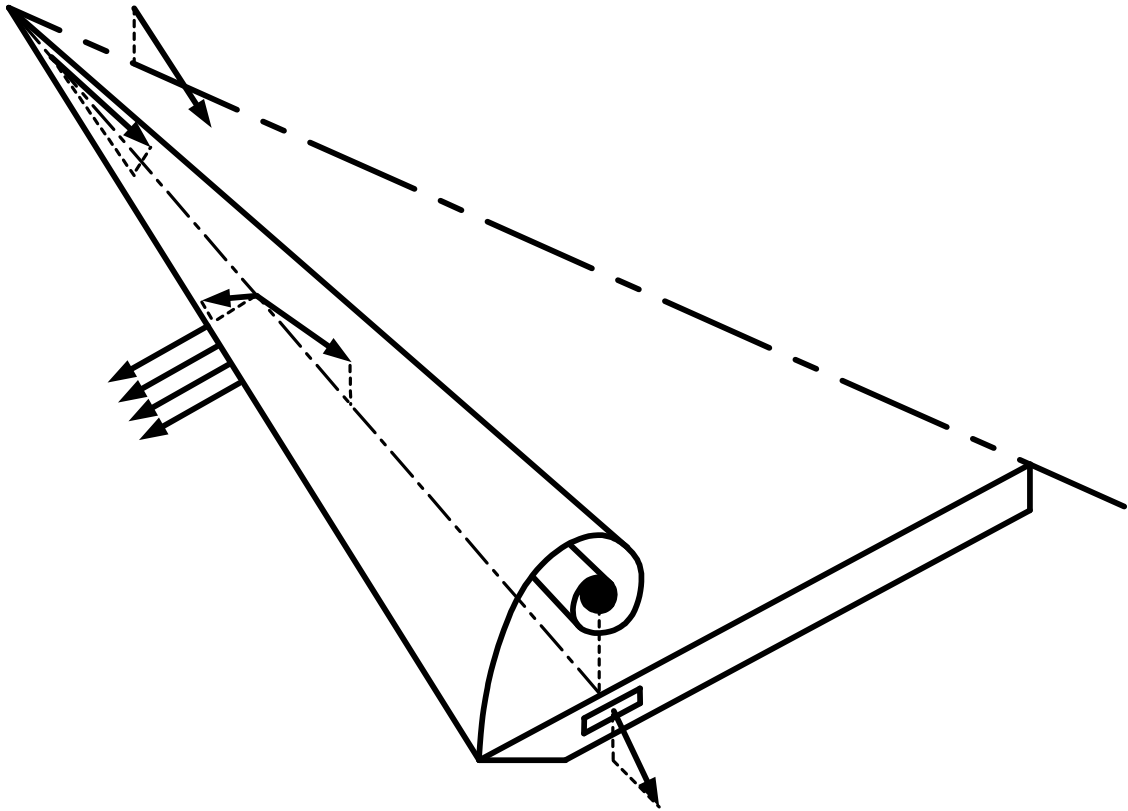


Figure 12: Schematic of various blowing configurations on a delta wing [44].

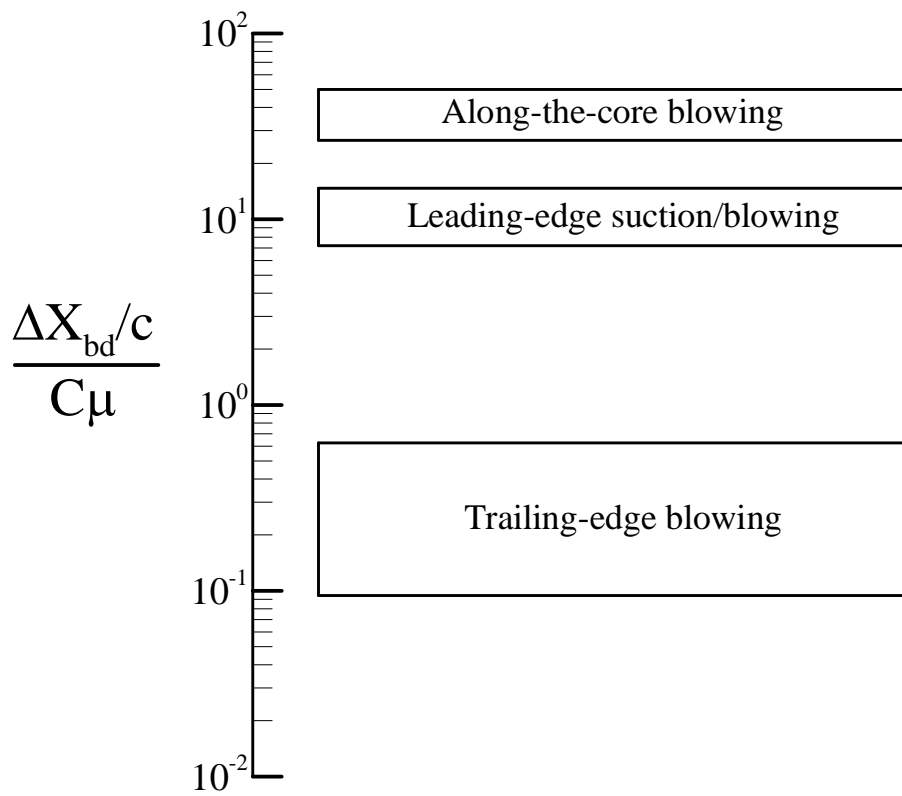
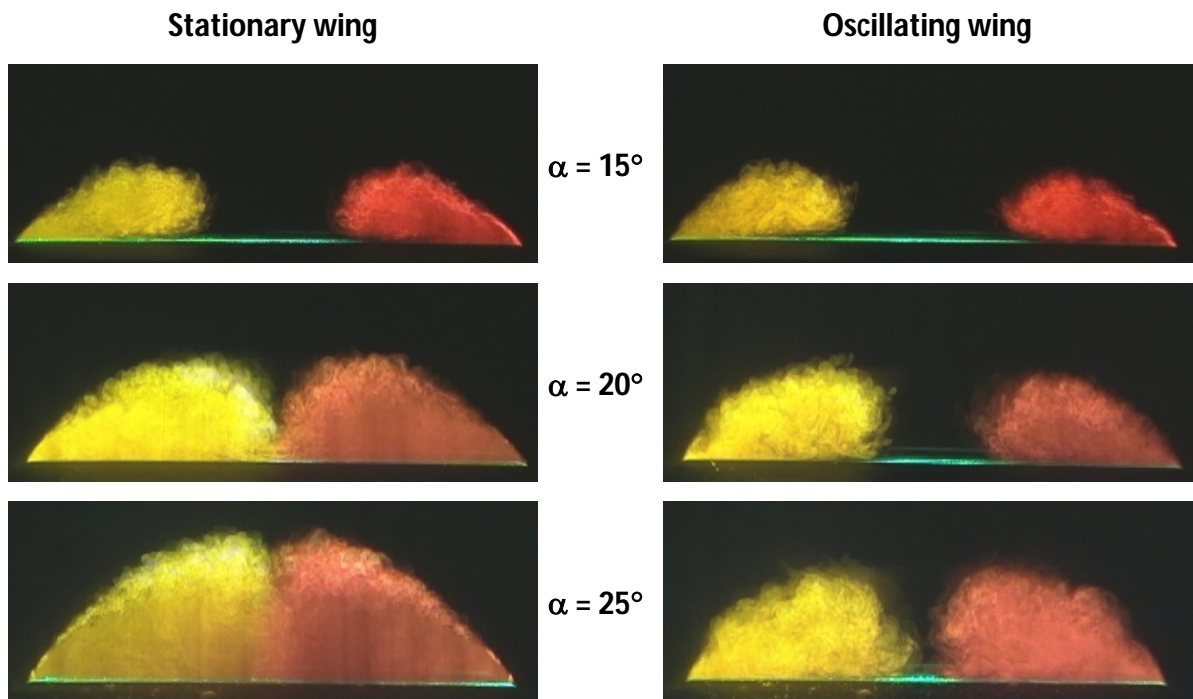


Figure 13: Effectiveness of various blowing methods [44].

(a)



(b)

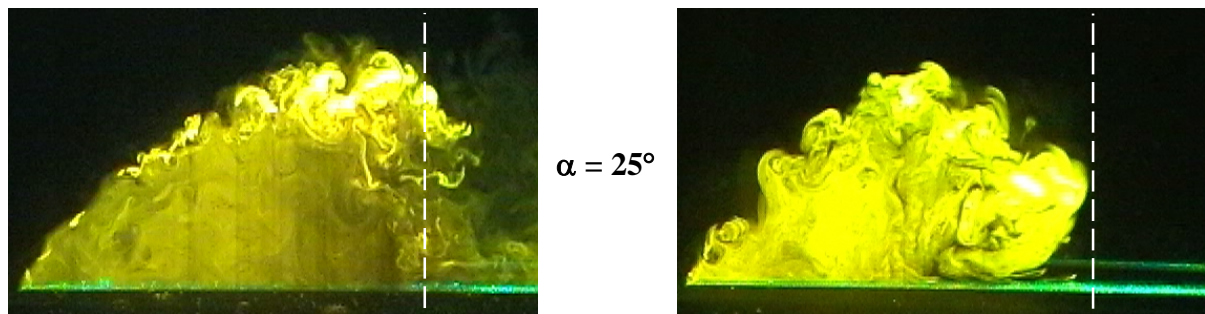


Figure 14: Visualization of (a) time-averaged vortices, (b) instantaneous flow [44].

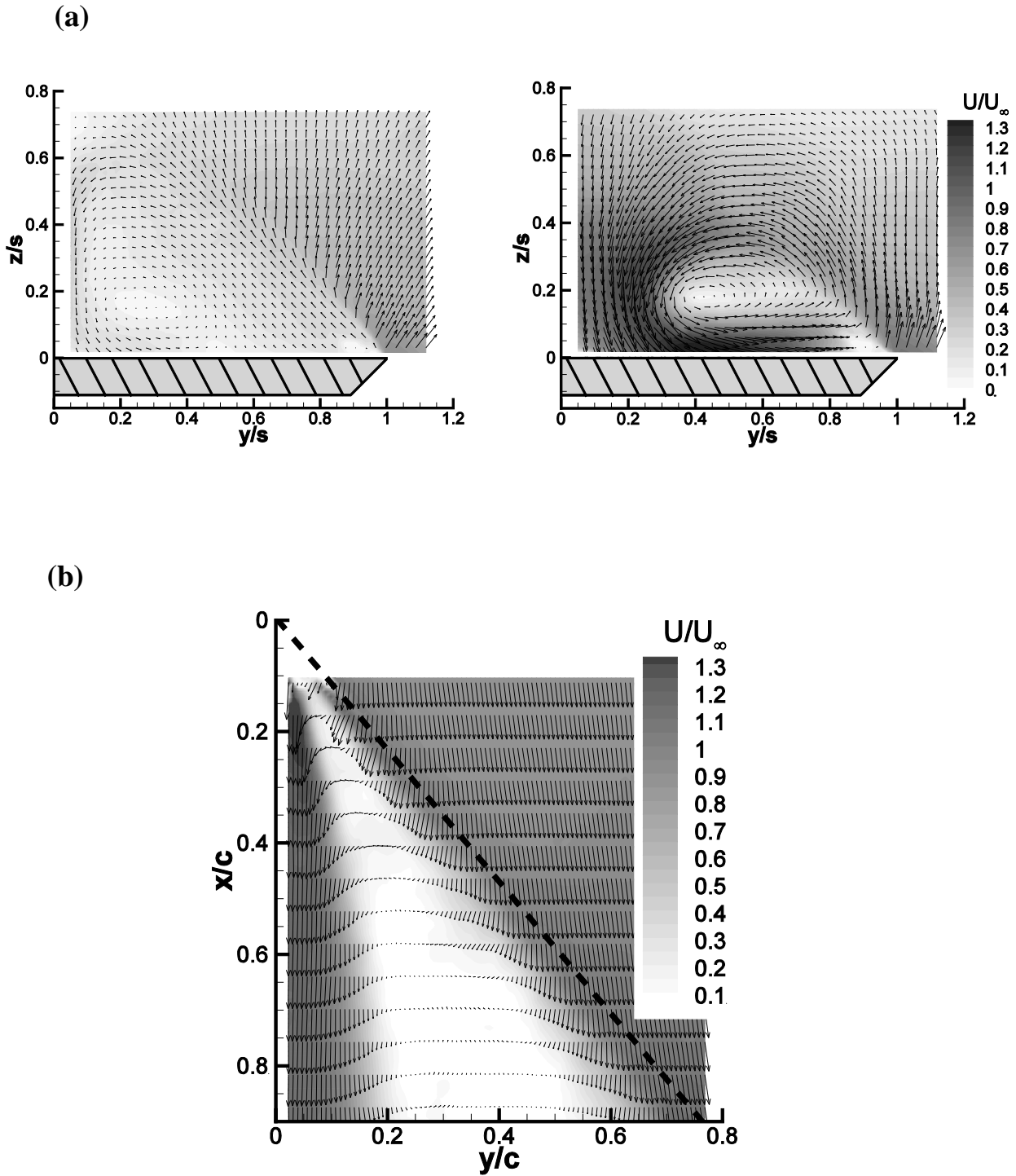


Figure 15: Time-averaged velocity (a) in the crossflow plane for the baseline case and with flow control ($C_{\mu}=0.26\%$), (b) in the plane through the vortex axis with flow control [29].

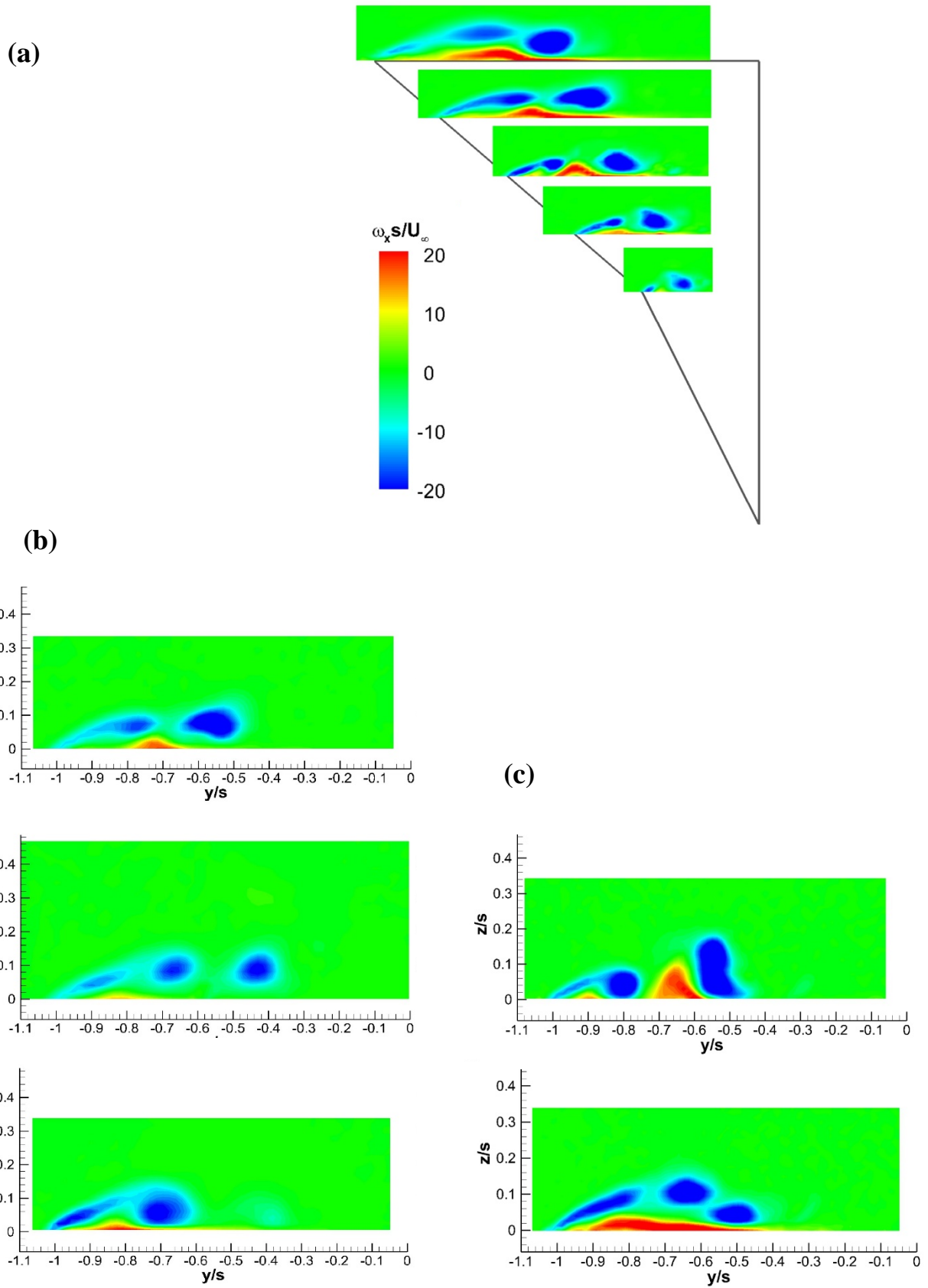


Figure 16: Time-averaged vorticity for (a) double delta wing, (b) baseline case and two different jet yaw angles, (c) two different bleed hole locations [34].

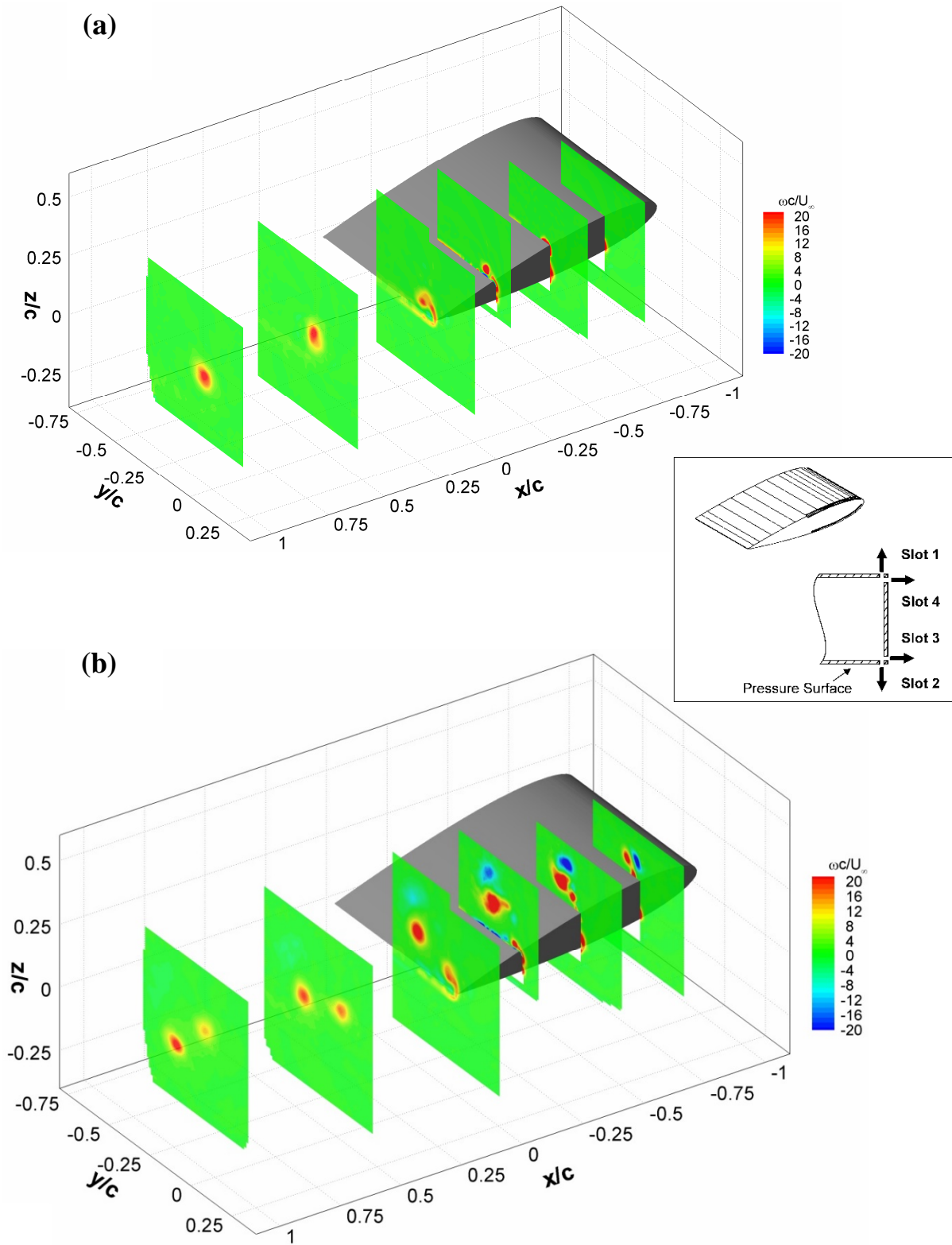


Figure 17: Vorticity field for (a) baseline case, (b) blowing from Slot 1, $C_\mu = 1\%$ [1].

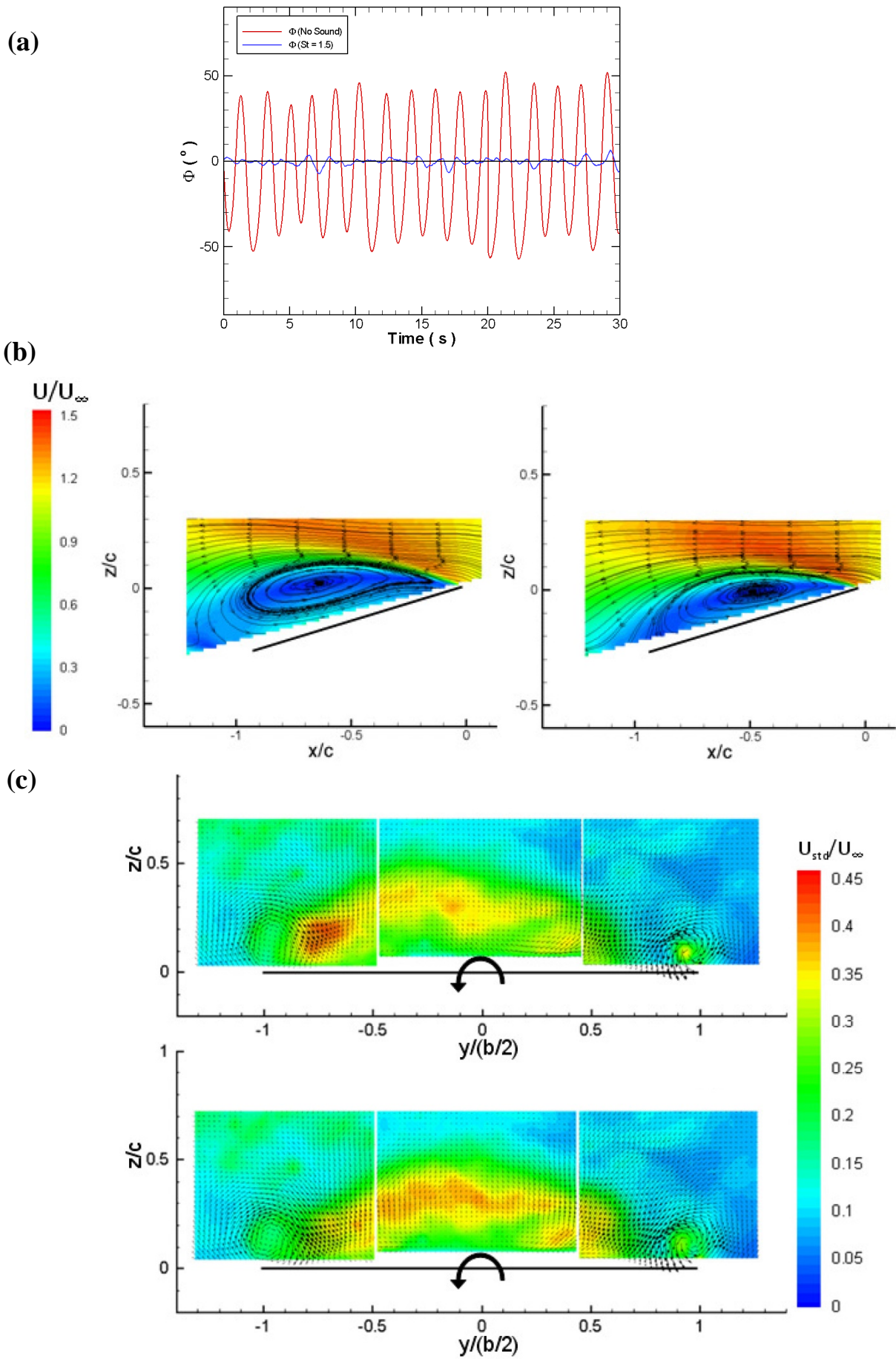


Figure 18: (a) Time history of roll angle for the baseline case and with acoustic excitation, (b) time-averaged flow in a plane parallel to the freestream with and without excitation, (c) velocity vectors and standard deviation of velocity in a crossflow plane with and without excitation [56].

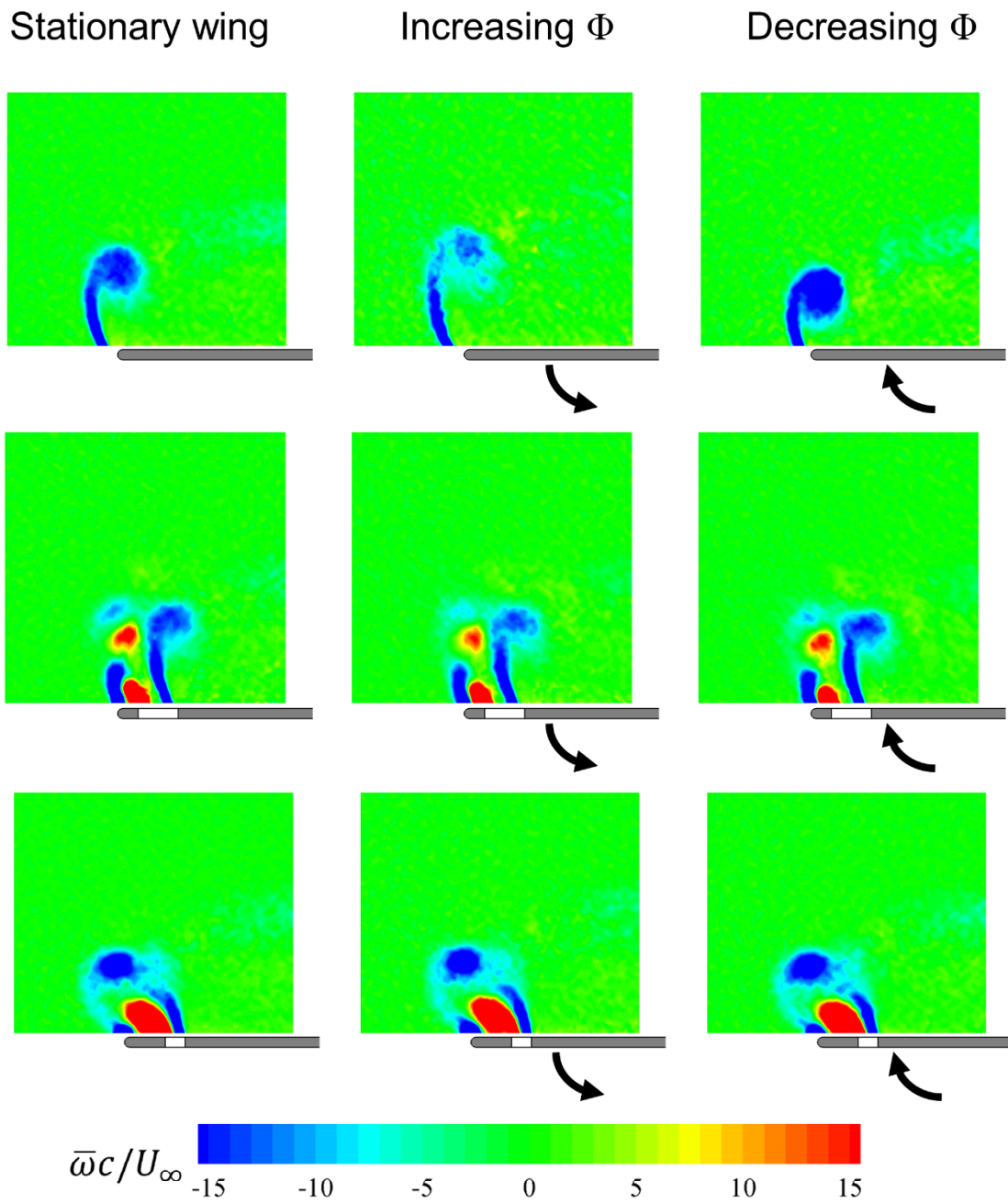


Figure 19: Phase-averaged streamwise vorticity for the baseline wing (top) and two bleed slot geometries (middle and bottom) [32].

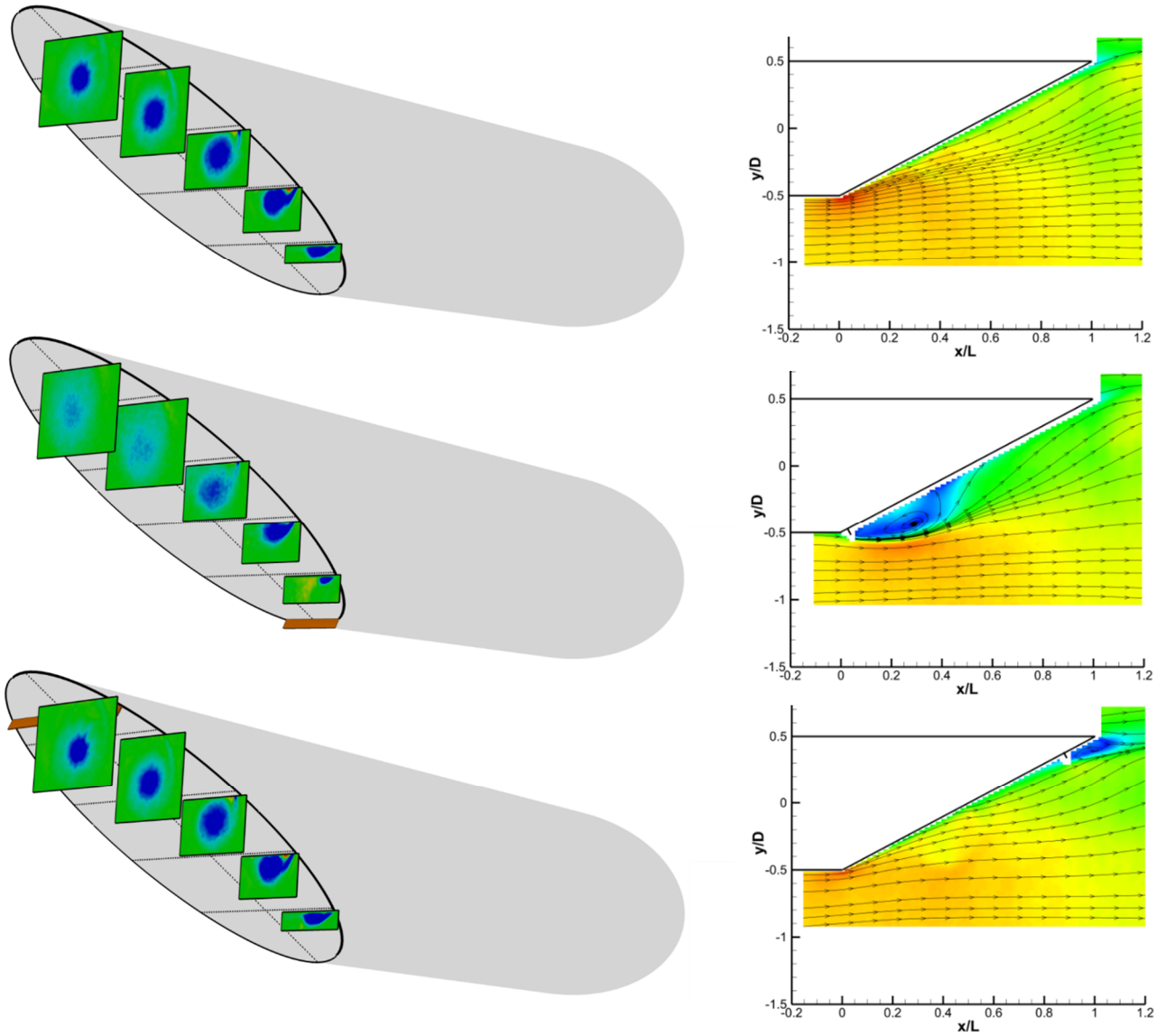


Figure 20: Baseline case (top) and two different locations of the mini-spoiler (middle and bottom): time-averaged vorticity (left) and velocity in the symmetry plane (right) [62].

(a)

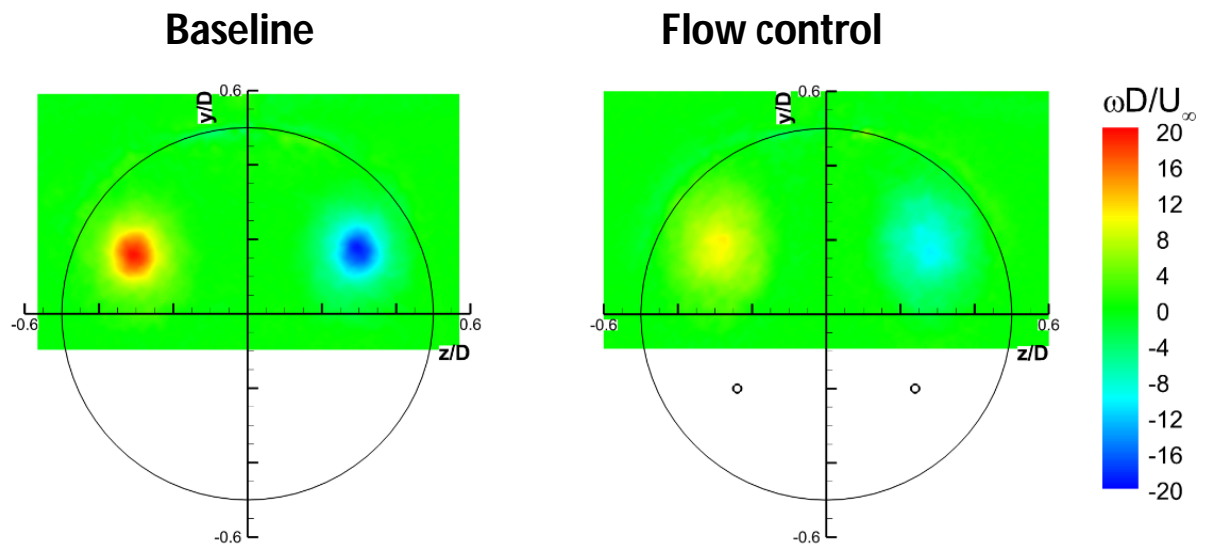
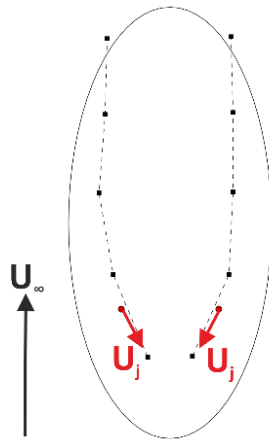
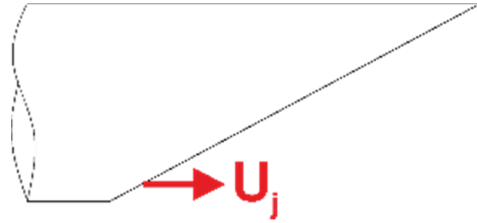
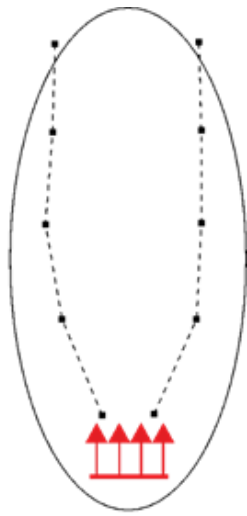


Figure 21: Streamwise vorticity for (a) vortex control with upstream blowing; (b) jet flap that reduces the drag [63].

(b)



Baseline

Flow control

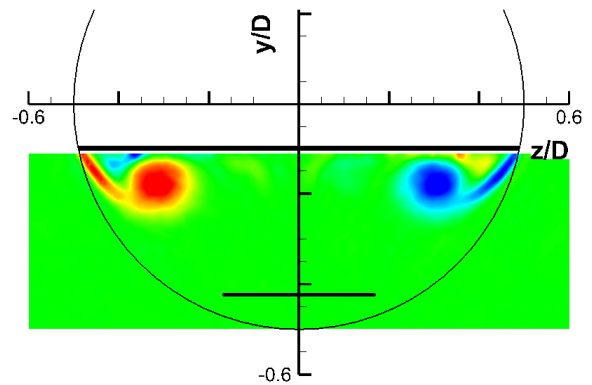
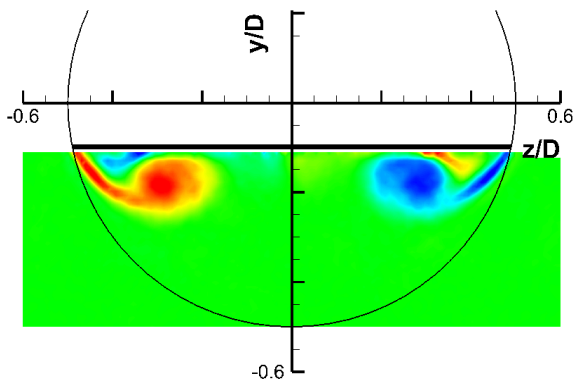
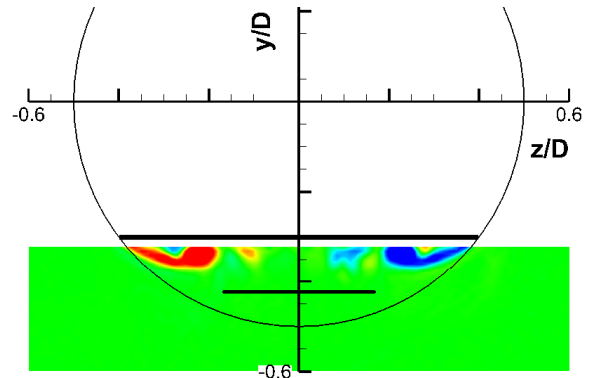
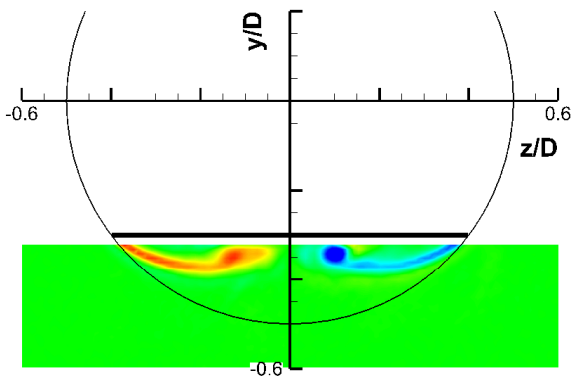


Figure 21: Continued.